

## General Disclaimer

### One or more of the Following Statements may affect this Document

- This document has been reproduced from the best copy furnished by the organizational source. It is being released in the interest of making available as much information as possible.
- This document may contain data, which exceeds the sheet parameters. It was furnished in this condition by the organizational source and is the best copy available.
- This document may contain tone-on-tone or color graphs, charts and/or pictures, which have been reproduced in black and white.
- This document is paginated as submitted by the original source.
- Portions of this document are not fully legible due to the historical nature of some of the material. However, it is the best reproduction available from the original submission.

TR-250-1400  
MARCH 1975

NASA CR-144002

# **ANALYTICAL STABILITY AND SIMULATION RESPONSE STUDY FOR A COUPLED TWO-BODY SYSTEM**

(NASA-CR-144002) ANALYTICAL STABILITY AND  
SIMULATION RESPONSE STUDY FOR A COUPLED  
TWO-BODY SYSTEM (Northrop Services, Inc.,  
Huntsville, Ala.) 86 p HC \$4.75 CACL 20K

N76-10504

Unclas  
03935

G3/39

PREPARED FOR:

**NATIONAL AERONAUTICS AND SPACE ADMINISTRATION  
GEORGE C. MARSHALL SPACE FLIGHT CENTER  
Science and Engineering Directorate**

Under Contract NAS8-29627



**NORTHROP SERVICES, INC.**

P. O. BOX 1384  
HUNTSVILLE, ALABAMA 35807  
TELEPHONE (205) 837-0580

**ANALYTICAL STABILITY AND SIMULATION RESPONSE STUDY  
FOR A COUPLED TWO-BODY SYSTEM**

March 1975

by

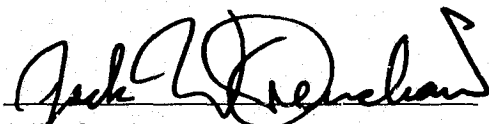
Kuoting M. Tao  
James R. Roberts

**PREPARED FOR:**

**NATIONAL AERONAUTICS AND SPACE ADMINISTRATION  
GEORGE C. MARSHALL SPACE FLIGHT CENTER  
SCIENCE AND ENGINEERING DIRECTORATE  
SYSTEMS DYNAMICS LABORATORY**

**Under Contract NAS8-29627**

**REVIEWED AND APPROVED BY:**



J. W. Crenshaw,  
Principal Investigator



M. A. Sloan, Jr., Manager  
Dynamics and Control Section

**FOREWORD**

This document was prepared by Northrop Services Inc., Huntsville, Alabama, for the Systems Dynamics Laboratory of the Science and Engineering Directorate of Marshall Space Flight Center, Huntsville, Alabama. Technical coordination was maintained through Mr. Mario H. Rheinfurth of the Dynamics and Trajectory Branch (ED15), and Mr. Pat Vallely and Ms. Alberta King of the Servo Mechanisms and Systems Stability Branch (ED14). The material presented herein is the result of work performed under Contract NAS8-29627 and is submitted as an interim report in response to the requirements of the said contract.

**ABSTRACT**

This report documents both an analytical stability study and a digital simulation response study of two connected rigid bodies. Relative rotation of the bodies at the connection is allowed, thereby providing a model suitable for studying system stability and response during a soft-dock regime. Provisions are made for a docking port axes alignment torque and a despin torque capability for encountering spinning payloads. Although the stability analysis is based on linearized equations, the digital simulation is based on nonlinear models.

**TABLE OF CONTENTS**

<u>Section</u>	<u>Title</u>	<u>Page</u>
	FOREWORD . . . . .	ii
	ABSTRACT . . . . .	iii
	LIST OF ILLUSTRATIONS . . . . .	vi
	LIST OF TABLES . . . . .	vii
I	INTRODUCTION . . . . .	1-1
	PART I - ANALYTICAL STABILITY ANALYSIS	
II	INTRODUCTION TO THE ANALYTICAL STABILITY ANALYSIS . . . . .	2-1
	2.1 GENERAL . . . . .	2-1
	2.2 VEHICLE ATTITUDE CONTROL, ALIGNMENT, AND DESPIN TORQUE OPTIONS . . . . .	2-3
	2.3 NOMINAL PARAMETERS FOR THE TWO-BODY MODEL . . . . .	2-5
III	LINEARIZED EQUATIONS OF MOTION AND STATE VARIABLE CANONICAL FORM . . . . .	3-1
	3.1 LINEARIZED EQUATIONS OF MOTION . . . . .	3-1
	3.2 JOINT TORQUE/ALIGNMENT AND DESPIN . . . . .	3-3
	3.3 REDUCED EQUATIONS OF MOTION AND STATE VARIABLE CANONICAL FORM . . . . .	3-6
IV	A-1 CONTROL OPTION - BODY 1 HAS THREE AXIS ATTITUDE CONTROL . . . . .	4-1
	4.1 REDUCED EQUATIONS OF MOTION . . . . .	4-1
	4.2 LINEAR MODEL OPEN-LOOP BEHAVIOR, DECOMPOSITION, AND INTERPRETATION . . . . .	4-3
	4.3 LINEAR MODEL CLOSED-LOOP BEHAVIOR . . . . .	4-8
	4.4 SOME STRUCTURAL PROPERTIES, PERFORMANCE EVALUATION, AND GENERAL DESIGN GUIDELINE . . . . .	4-10
V	A-2/A-3 CONTROL OPTION - BODY 1 HAS X-AXIS ONLY OR NO ATTITUDE CONTROL . . . . .	5-1
	5.1 LINEAR MODEL OPEN-LOOP BEHAVIOR, DECOMPOSITION, AND INTERPRETATION . . . . .	5-1
	5.2 LINEAR MODEL CLOSED-LOOP BEHAVIOR . . . . .	5-4
	5.3 SOME STRUCTURAL PROPERTIES, PERFORMANCE EVALUATION, AND GENERAL DESIGN GUIDELINE . . . . .	5-7
	5.4 EFFECTS OF INITIAL ANGULAR SPEED MATCHING . . . . .	5-17

## TABLE OF CONTENTS (Concluded)

<u>Section</u>	<u>Title</u>	<u>Page</u>
VI	ABSOLUTE STABILITY AND THE STABILITY REGION OF THE SPRING/DAMPER COMPENSATED COUPLED TWO-BODY SYSTEM . . . . .	6-1
	PART II - SIMULATION RESPONSE STUDY	
VII	SIMULATION RESPONSE STUDY . . . . .	7-1
	7.1 GENERAL . . . . .	7-1
	7.2 SIMULATION RESULTS . . . . .	7-1
VIII	SUMMARY, CONCLUSIONS, AND DISCUSSION . . . . .	8-1
IX	REFERENCES . . . . .	9-1
	APPENDIX A - GENERAL EQUATIONS OF MOTION FOR TWO COUPLED RIGID BODIES . . . . .	A-1
	APPENDIX B - SIMPLIFIED LINEARIZED EQUATIONS OF MOTION FOR TWO COUPLED RIGID BODIES . . . . .	B-1
	APPENDIX C - SIMPLIFIED LINEARIZED EQUATIONS OF MOTION FOR TWO COUPLED RIGID BODIES IN TERMS OF NEW VARIABLES . . . . .	C-1
	APPENDIX D - MATHEMATICAL MODELS USED IN THE 2BODY SIMULATION . . . . .	D-1

## LIST OF ILLUSTRATIONS

<u>Figure</u>	<u>Title</u>	<u>Page</u>
2-1	ROTATIONAL COORDINATES OF BODY $i$ . . . . .	2-1
2-2	DESPIN TORQUE MODEL. . . . .	2-4
4-1	COUPLED SYSTEM ROOT LOCUS DIAGRAM . . . . .	4-12
5-1	V-CANONICAL STRUCTURE MODEL . . . . .	5-7
5-2	SIMPLIFIED STRUCTURE I . . . . .	5-9
5-3	SIMPLIFIED STRUCTURE II . . . . .	5-14
5-4	ROOT LOCUS DIAGRAM . . . . .	5-16
6-1	STABILITY REGION ESTIMATION BY QUADRATIC LIAPUNOV FUNCTION .	6-2
6-2	GENERAL NONLINEAR STRUCTURE MODEL . . . . .	6-3
6-3	A DECOMPOSED VIEW . . . . .	6-5
7-1	TWO-BODY BEHAVIOR FOR UNCONTROLLED TUG . . . . .	7-2
7-2	TWO-BODY BEHAVIOR FOR TUG 3-AXIS ATTITUDE CONTROL . . . . .	7-3
7-3	DAMPING EFFECT . . . . .	7-5
7-4	ALIGNMENT NATURAL FREQUENCY EFFECT . . . . .	7-6
7-5	DESPIN TORQUE EFFECT . . . . .	7-7
D-1	TWO COUPLED RIGID BODIES INERTIALLY REFERENCED . . . . .	D-1
D-2	TWO COUPLED RIGID BODIES WITH IDEAL JOINT . . . . .	D-2
D-3	DESPIN TORQUER OUTPUT MODEL . . . . .	D-6



## LIST OF TABLES

<u>Table</u>	<u>Title</u>	<u>Page</u>
2-1	BODY 1 IDEAL ATTITUDE CONTROL OPTIONS . . . . .	2-4
2-2	ALIGNMENT AND/OR DESPIN TORQUE OPTIONS . . . . .	2-4
2-3	NOMINAL TWO-BODY MODEL . . . . .	2-5
4-1	OPEN LOOP POLES/WITH DESPIN TORQUE . . . . .	4-8
4-2	CLOSED-LOOP TIME CONSTANTS AND PERIODS/WITHOUT DESPIN TORQUE . . . . .	4-9
4-3	NUMERICAL DATA FOR FIGURE 4-1. . . . .	4-13
5-1	OPEN-LOOP POLES/WITH DESPIN TORQUE . . . . .	5-4
5-2	IMPORTANT POLE-PAIRS . . . . .	5-10
5-3	COUPLING FACTORS . . . . .	5-11
5-4	POLES, ZEROS, AND GAIN OF THE RESOLVENT MATRIX . . . . .	5-11
5-5	RESIDUES AND PHASE SHIFTS . . . . .	5-12
5-6	A COMPARISON OF ESTIMATED AND ACTUAL AMPLITUDES . . . . .	5-15
6-1	POLES FOR SMALL SPRING/DAMPER CONSTANTS . . . . .	6-6

## Section I

## INTRODUCTION

An important baseline mission of the Space Tug is the recovery of satellites at or below synchronous orbital altitudes for return to the Space Shuttle. Such recovery type missions for the Tug are to include the recovery of malfunctioning satellites. A probable malfunction is partial or complete loss of vehicle attitude control. The Tug must be able to dock and successfully capture with a high probability on the first attempt.

In order to assess the feasibility of recovering a spinning satellite that is in a stable spin, but lacks the capability to despin, a study is made of the stability and response of the post-dock configuration. That is, the vehicles are initially assumed to already be in a soft-dock regime wherein capture or initial latch has been achieved but final latch or hard-dock has not. This system configuration is modeled as two rigid bodies connected at a single point about which relative rotation is permitted. The spin axis of the satellite (payload) is restricted to lie in the vicinity of the docking port axis. The behavior of this system model is then assessed relative to mass/inertia characteristics, vehicle coupling through the docking mechanism (joint alignment torque), despin torquer limits for despinning the payload, and ideal 3-axis attitude control of the Tug.

A dual approach is taken to the above problem. First, an analytical stability study is made based primarily on a linearized model thereby enabling the utilization of such linear stability techniques as root locus. This analysis makes up Part I of this report and is presented in Sections II through VI. In Section II, an introduction to the analytical stability study is given. Secondly, a simulation response study based on a nonlinear system model is presented in Part II (or Section VII). Finally, in Section VIII a summary of results for both the analytical and simulation study are presented along with conclusions and some discussion.

## Section II

## INTRODUCTION TO THE ANALYTICAL STABILITY ANALYSIS

## 2.1 GENERAL

Upon considering two rigid bodies connected at a single point and each spinning primarily along its body x-axis, it is only natural to be concerned with the relative motion between the x-axes of the two bodies. If an initial misalignment between these two axes continually grows with increasing time, then the coupled spinning body system is said to be unstable. In this context, "stability" is taken to mean the stability of the misalignment angle between the two-body spinning axes and it is readily seen that this misalignment angle is directly related to the y and z-directional rotations of each body, that is  $\theta_{1y}$ ,  $\theta_{1z}$ ,  $\theta_{2y}$ , and  $\theta_{2z}$ . In Figure 2-1, the Euler angles  $\theta_{ix}$ ,  $\theta_{iy}$ , and  $\theta_{iz}$  ( $i = 1, 2$ ) are illustrated for a 3-2-1 (z-y-x) rotation sequence. It is seen that the position of the  $x_i$ -axis is located relative to the inertial reference frame X, Y, Z by two angles  $\theta_{iy}$  and  $\theta_{iz}$ .

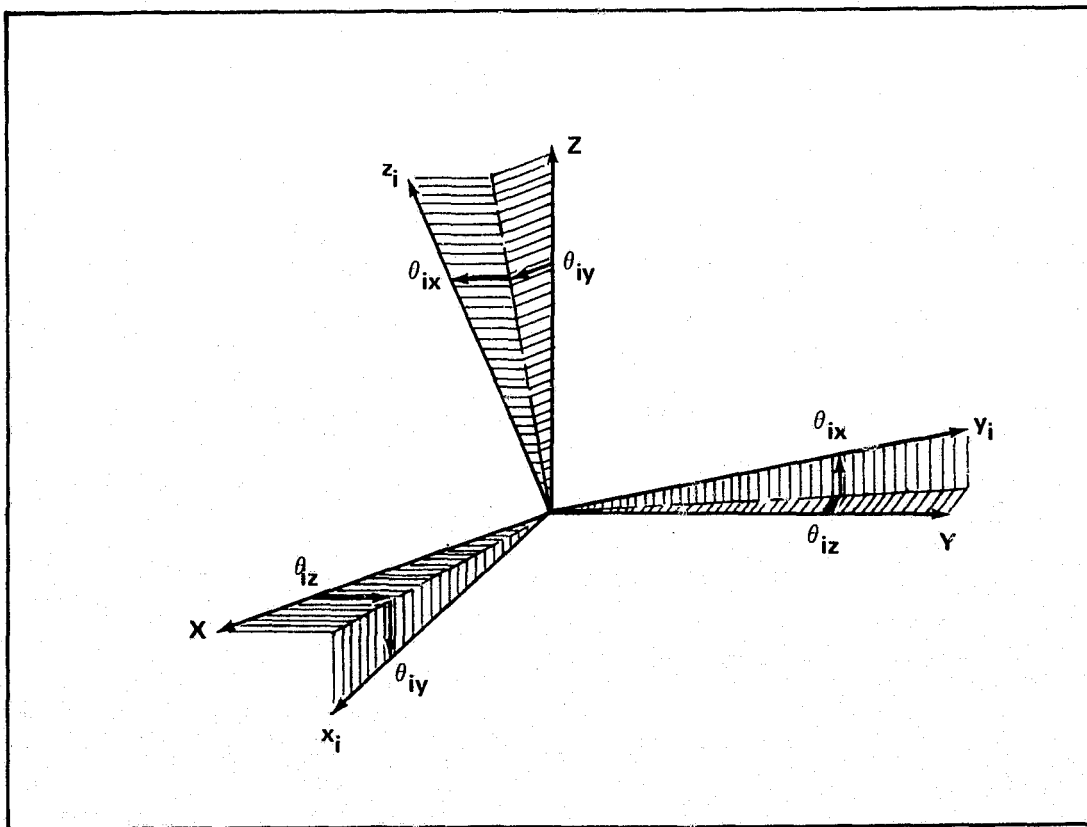


Figure 2-1. ROTATIONAL COORDINATES OF BODY i

As with most cases in nature, this is a nonlinear system with state variables intermingled, thereby complicating the stability analysis. Although such theories as Popov's criterion and Liapunov's second method exist for nonlinear system stability analysis, they are either not suitable for this specific problem or difficult to apply. Consequently, a more popular and easier method known as "linearization" is adopted even though it is often times less powerful than Liapunov's second method.

The idea is to study the linear effect of perturbation around an equilibrium operation point in the state space. If, in addition to the previously stated assumption that the two bodies are spinning primarily along their body x-axes, the y and z-directional rotations are assumed small, then the equilibrium operation point becomes obvious, namely that for which each body is spinning only about its x-axis and the y and z-directional rotations are null (perfect alignment between the body fixed reference frames). Thus

$$\theta_{1y} = \theta_{1z} = \theta_{2y} = \theta_{2z} = 0$$

and

$$\dot{\theta}_{1y} = \dot{\theta}_{1z} = \dot{\theta}_{2y} = \dot{\theta}_{2z} = 0 .$$

By dropping out all of the second and higher order terms involving  $\theta_{1y}$ ,  $\theta_{1z}$ ,  $\theta_{2y}$ ,  $\theta_{2z}$ ,  $\dot{\theta}_{1y}$ ,  $\dot{\theta}_{1z}$ ,  $\dot{\theta}_{2y}$ , and  $\dot{\theta}_{2z}$ , an appropriate linearized system of equations is obtained (see Section III). A study of these linearized equations of motion would then hopefully reveal the stability of the original nonlinear system.

The theoretical foundation of this linear analysis is Liapunov's first method (refs. 1, 2), which can be summarized as follows:

- If the linearized system is asymptotically stable, the (asymptotic) stability of the nonlinear system is assured.
- If the linearized system is unstable, the nonlinear system is also unstable.
- If the linearized system is stable but not asymptotically stable, the stability of the nonlinear system will be determined by higher order terms.

For a free-spinning two-body system (one for which no external environmental torques or stabilization devices are considered), it is quite possible that the linearized model cannot determine nonlinear stability. However, the objective of the study is to learn how to drive the misalignment angles close to zero in a reasonably short time, that is, to control the system to be asymptotically stable. Since a spring and damper are to be used to align and stabilize the x-axes of the spinning system, it is expected that the linearized model will prove to be both a powerful and convenient tool for analysis.

There is still another question which remains to be answered, that concerning the "region of stability." The stability region is defined as the maximum region in the state space for which any initial condition will result in a trajectory that approaches the equilibrium point with increasing time. It should be noted that, in general, nonlinear asymptotic stability is only a local property rather than global, although linear stability is always global. Unfortunately, Liapunov's first method cannot provide any information on the stability region and this question must then be investigated separately.

## 2.2 VEHICLE ATTITUDE CONTROL, ALIGNMENT, AND DESPIN TORQUE OPTIONS

For both demonstrative and practical purposes, a number of operational conditions relative to vehicle attitude control, alignment, and despin torque are to be considered in the analytical stability study. Relative to vehicle attitude control (A), there are three options which can be imposed on body 1. These are given in Table 2-1. For the A-2 control option, the desired connotation of "x-axis only" attitude control is implied by the condition  $\dot{\theta}_{1x} = 0$ . Although the A-3 control option indicates no attitude control, this does not preclude the possibility of body 1 having an initial spin rate identical to that of body 2. In addition, there are four options available relative to an alignment and/or despin torque (L). These are presented in Table 2-2. Together, Tables 2-1 and 2-2 form a matrix of 12 operational conditions to consider. It should be noted that L-1 and L-2 are open-loop options whereas L-3 and L-4 are closed loop options.

Table 2-1. BODY 1 IDEAL ATTITUDE CONTROL OPTIONS

A-1	Body 1 has ideal "3-axis" attitude control
A-2	Body 1 has ideal "x-axis only" attitude control
A-3	Body 1 has "no" attitude control

Table 2-2. ALIGNMENT AND/OR DESPIN TORQUE OPTIONS

L-1	Without alignment torque/without despin torque
L-2	Without alignment torque/with despin torque
L-3	With alignment torque/without despin torque
L-4	With alignment torque/with despin torque

In the following analytical stability study, a simple but practical model for the despin torque is used. For the A-1 and A-2 control options, a constant x-directional despin torque ( $L_D$ ) is assumed to be acting as long as the x-directional relative spin rate between the two bodies ( $\Delta\omega$ ) is not zero (see Figure 2-2).

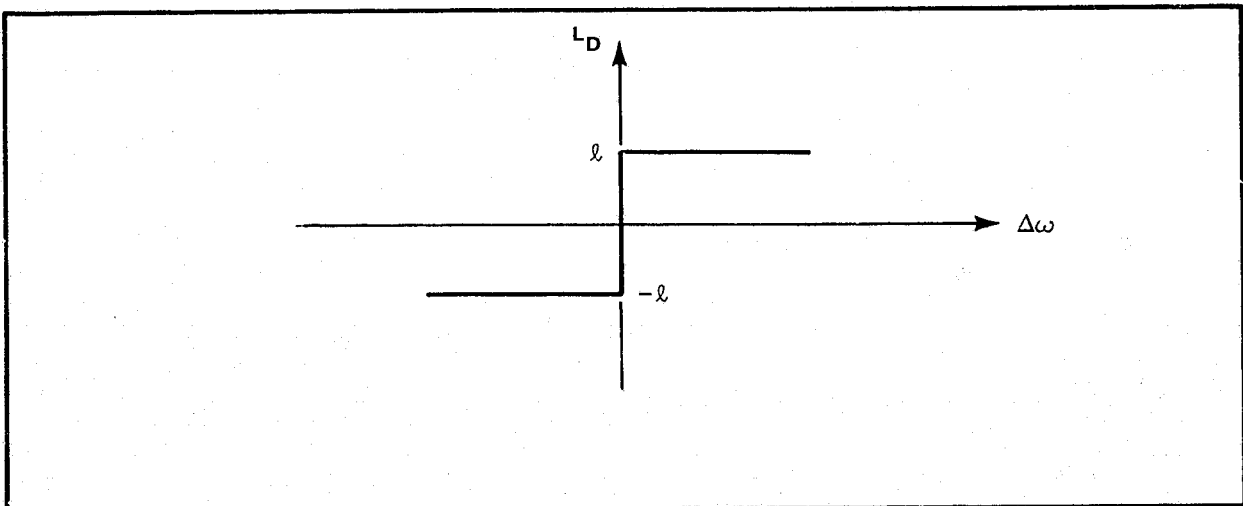
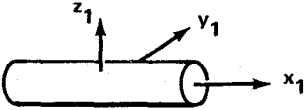
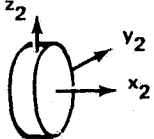


Figure 2-2. DESPIN TORQUE MODEL

2.3 NOMINAL PARAMETERS FOR THE TWO-BODY MODEL

In the following study, analysis and design is based on a "nominal model" with variant models examined as necessary. Table 2-3 presents the parameters defining the configuration of the "nominal" two-body model.

Table 2-3. NOMINAL TWO-BODY MODEL

	Body 1 (Tug)	Body 2 (Spinning Satellite)
Shape		
Mass	$m_1 = 3222 \text{ Kg}$	$m_2 = 4500 \text{ Kg}$
Inertia	$A_1 = 8418 \text{ Kg-m}^2$ $B_1 = C_1 = 31000 \text{ Kg-m}^2$	$A_2 = 43400 \text{ Kg-m}^2$ $B_2 = C_2 = 11732 \text{ Kg-m}^2$
Joint Vector	$d_{1x} = 5 \text{ m}$ $d_{1y} = d_{1z} = 0$	$d_{2x} = -2.3 \text{ m}$ $d_{2y} = d_{2z} = 0$

Each body is assumed to be symmetrical about the body x-axis with respect to inertia resulting in an inertia matrix of the form

$$I_i = \begin{bmatrix} A_i & 0 & 0 \\ 0 & C_i & 0 \\ 0 & 0 & C_i \end{bmatrix}, \quad i = 1, 2$$

The bodies are assumed to be homogenous thereby requiring the center of mass of each body to lie on the x-axis. In addition, the joint connecting the two bodies is assumed to lie on the x-axis of each body resulting in a joint vector (vector from the center of mass to the joint) for each body of the form

$$d_i = \begin{bmatrix} d_{ix} \\ 0 \\ 0 \end{bmatrix}, \quad i = 1, 2 .$$

The nominal value of the initial spin rate of body 2 is 0.1 rad/sec along the  $x_2$ -axis.



## Section III

## LINEARIZED EQUATIONS OF MOTION AND STATE VARIABLE CANONICAL FORM

## 3.1 LINEARIZED EQUATIONS OF MOTION

In Appendix A, a derivation is given for the nonlinear equations of motion for two rigid bodies connected at a single point. In Appendix B, these nonlinear equations of motion are simplified according to the following assumptions:

- No external environmental forces or torques are acting on the bodies.
- Partial linearization: The rotations about the y and z-axes of both bodies are assumed small as well as the products of these angles and their rates.
- Both bodies are symmetrical about the body x-axis with respect to inertia.
- The center of mass of each body is located on its respective body x-axis.
- The joint or connection between the bodies is located on the x-axis of each body.

Based on these assumptions, the resulting two-body equations of motion are given by

$$\hat{J} \ddot{\theta} + \hat{K} \dot{\theta} = \hat{L} \quad (3-1)$$

with

$$\hat{J} = \begin{bmatrix} C_1^* & 0 & -K & 0 \\ 0 & C_1^* & 0 & -K \\ -K & 0 & C_2^* & 0 \\ 0 & -K & 0 & C_2^* \end{bmatrix},$$

$$\hat{K} = \begin{bmatrix} 0 & A_1 \dot{\theta}_{1x} & 0 & 0 \\ -A_1 \dot{\theta}_{1x} & 0 & 0 & 0 \\ 0 & 0 & 0 & A_2 \dot{\theta}_{2x} \\ 0 & 0 & -A_2 \dot{\theta}_{2x} & 0 \end{bmatrix},$$

$$\ddot{\theta} = \begin{bmatrix} \ddot{\theta}_{1y} \\ \ddot{\theta}_{1z} \\ \ddot{\theta}_{2y} \\ \ddot{\theta}_{2z} \end{bmatrix}, \quad \dot{\theta} = \begin{bmatrix} \dot{\theta}_{1y} \\ \dot{\theta}_{1z} \\ \dot{\theta}_{2y} \\ \dot{\theta}_{2z} \end{bmatrix}, \quad \text{and} \quad \hat{L} = \begin{bmatrix} \hat{L}_{1y} \\ \hat{L}_{1z} \\ -\hat{L}_{2y} \\ -\hat{L}_{2z} \end{bmatrix}$$

where

$$\left. \begin{aligned} \hat{L}_{iy} &= L_{iy} \cos \theta_{ix} - L_{iz} \sin \theta_{ix} \\ \hat{L}_{iz} &= L_{iy} \sin \theta_{ix} + L_{iz} \cos \theta_{ix} \\ C_i^* &= C_i + m^* d_i^2 \end{aligned} \right\} \quad i = 1, 2$$

$$K = m^* d_1 d_2$$

$$m^* = \frac{m_1 m_2}{m_1 + m_2}$$

and

- $A_1, A_2$  - principal x-axis inertia of body 1, 2
- $C_1, C_2$  - principal y and z-axis inertia of body 1, 2
- $d_1, d_2$  - distance along the x-axis from the body 1, 2 center of mass to the joint between the bodies
- $L_{iy}, L_{iz}$  - joint torque about the y and z axes of body i,  $i = 1, 2$
- $m_1, m_2$  - mass of body 1, 2
- $\theta_{ix}, \theta_{iy}, \theta_{iz}$  - body rotations about the x, y, and z axes of body i,  $i = 1, 2$
- $\dot{\theta}_{ix}, \dot{\theta}_{iy}, \dot{\theta}_{iz}$  - angular velocities of body i,  $i = 1, 2$
- $\ddot{\theta}_{ix}, \ddot{\theta}_{iy}, \ddot{\theta}_{iz}$  - angular accelerations of body i,  $i = 1, 2$

## 3.2 JOINT TORQUE/ALIGNMENT AND DESPIN

The joint torque,  $\underline{L}$ , as expressed in inertial space is given by

$$\underline{L} = T_1 \underline{L}_1 = T_2 \underline{L}_2$$

where  $T_1$  and  $T_2$  are the coordinate transformation matrices resolving body 1 and 2 coordinates, respectively, into the inertial reference frame (see Appendix B for the derivation of  $T_1$  and  $T_2$ ). To a first order approximation, the joint torque expressed in the inertial frame is then given by

$$\underline{L}_i = \begin{bmatrix} L_{ix} \\ L_{iy} \\ L_{iz} \end{bmatrix} = \begin{bmatrix} L_{ix} \\ L_{ix} \theta_{iz} + L_{iy} \cos \theta_{ix} - L_{iz} \sin \theta_{ix} \\ -L_{ix} \theta_{iy} + L_{iy} \sin \theta_{ix} + L_{iz} \cos \theta_{ix} \end{bmatrix}, \quad i = 1, 2.$$

Comparison of this equation to those defined in subsection 3.1 for  $L_{iy}$  and  $L_{iz}$  results in

$$\hat{L}_{iy} = L_y - L_x \theta_{iz}$$

and

(3-2)

$$\hat{L}_{iz} = L_z + L_x \theta_{iy}$$

which will prove useful in subsection 3.3.

The joint torque results from two separate sources, namely an alignment torque or spring-damper feedback that will tend to align the x-axes of the two bodies and a despin torque which will be applied to the x-axis of one of the bodies for despinning. In general then, the alignment torque ( $\underline{L}_A$ ) and the despin torque ( $\underline{L}_D$ ) as resolved in body  $i$  will have the form

$$\underline{L}_{Ai} = \begin{bmatrix} 0 \\ L_{Aiy} \\ L_{Aiz} \end{bmatrix}, \quad \underline{L}_{Di} = \begin{bmatrix} L_{Dix} \\ 0 \\ 0 \end{bmatrix}, \quad i = 1, 2$$

and the joint torque is then defined by

$$\underline{L} = \underline{L}_A + \underline{L}_D .$$

Based on the despin torque model presented in subsection 2.2, the despin torque acting on body  $i$  can be written as

$$\underline{L}_{Di} = \ell \hat{i}_i , \quad i = 1, 2$$

where

$\ell$  - magnitude of the despin torque (see Figure 2-1)  
 $\hat{i}_i$  - x-axis unit vector of body  $i$

then

$$\underline{L}_{Di} = \ell T_i \hat{i}_i$$

or

$$\underline{L}_{Di} = \ell \begin{bmatrix} T_{i11} \\ T_{i21} \\ T_{i31} \end{bmatrix} = \ell \begin{bmatrix} 1 \\ \theta_{iz} \\ -\theta_{iy} \end{bmatrix} , \quad i = 1, 2 \quad (3-3)$$

To damp the scissoring-type angular motion between the bodies, an alignment or spring-damper feedback torque of the form

$$\underline{L}_A = k \underline{v} + \lambda \dot{\underline{v}}$$

is provided where  $k$  and  $\lambda$  are spring and damper coefficients and  $\underline{v}$  is an error vector based on the amount of angular misalignment between the x-axes of the two bodies. That is,

$$\underline{v} = \hat{i}_1 \times \hat{i}_2$$

which, when resolved into the inertial reference frame becomes

$$\underline{v} = T_1 \hat{i}_1 \times T_2 \hat{i}_2$$

$$= \begin{bmatrix} T_{111} \\ T_{121} \\ T_{131} \end{bmatrix} \times \begin{bmatrix} T_{211} \\ T_{221} \\ T_{231} \end{bmatrix} = \begin{bmatrix} 1 \\ \theta_{1z} \\ -\theta_{1y} \end{bmatrix} \times \begin{bmatrix} 1 \\ \theta_{2z} \\ -\theta_{2y} \end{bmatrix}$$

$$\underline{v} = \begin{bmatrix} \theta_{1y}\theta_{2z} - \theta_{1z}\theta_{2y} \\ \theta_{2y} - \theta_{1y} \\ \theta_{2z} - \theta_{1z} \end{bmatrix} \approx \begin{bmatrix} 0 \\ \theta_{2y} - \theta_{1y} \\ \theta_{2z} - \theta_{1z} \end{bmatrix} .$$

If two new coordinates are defined as

$$\eta = \theta_{2y} - \theta_{1y}$$

and

$$\zeta = \theta_{2z} - \theta_{1z}$$

then

$$\underline{v} = \begin{bmatrix} 0 \\ \eta \\ \zeta \end{bmatrix}$$

and

$$\dot{\underline{v}} = \begin{bmatrix} 0 \\ \dot{\eta} \\ \dot{\zeta} \end{bmatrix} .$$

Therefore,

$$\underline{L}_A = k \begin{bmatrix} 0 \\ \eta \\ \zeta \end{bmatrix} + \lambda \begin{bmatrix} 0 \\ \dot{\eta} \\ \dot{\zeta} \end{bmatrix}$$

or

$$\underline{L}_A = \begin{bmatrix} L_{Ax} \\ L_{Ay} \\ L_{Az} \end{bmatrix} = \begin{bmatrix} 0 \\ k\eta + \lambda\dot{\eta} \\ k\zeta + \lambda\dot{\zeta} \end{bmatrix} \quad (3-4)$$

### 3.3 REDUCED EQUATIONS OF MOTION AND STATE VARIABLE CANONICAL FORM

In Appendix C, the simplified two-body equations of motion as given by equation (3-1) are even further reduced by making a change of variables. These reduced two-body equations of motion are

$$\begin{bmatrix} \ddot{Y} \\ \ddot{Z} \\ \ddot{\eta} \\ \ddot{\zeta} \end{bmatrix} + \begin{bmatrix} 0 & p_1 & 0 & -p_2 \\ -p_1 & 0 & p_2 & 0 \\ 0 & -p_3 & 0 & p_4 \\ p_3 & 0 & -p_4 & 0 \end{bmatrix} \begin{bmatrix} \dot{Y} \\ \dot{Z} \\ \dot{\eta} \\ \dot{\zeta} \end{bmatrix} = \begin{bmatrix} (\hat{L}_{1y} - \hat{L}_{2y})/(a_1 + a_2) \\ (\hat{L}_{1z} - \hat{L}_{2z})/(a_1 + a_2) \\ -(a_2 \hat{L}_{1y} + a_1 \hat{L}_{2y})/\Delta \\ -(a_2 \hat{L}_{1z} + a_1 \hat{L}_{2z})/\Delta \end{bmatrix} \quad (3-5)$$

with

$$\begin{aligned} Y &= \alpha\theta_{1y} + (1-\alpha)\theta_{2y} \\ Z &= \alpha\theta_{1z} + (1-\alpha)\theta_{2z} \\ \eta &= \theta_{2y} - \theta_{1y} \\ \zeta &= \theta_{2z} - \theta_{1z} \\ p_1 &= (A_1 \dot{\theta}_{1x} + A_2 \dot{\theta}_{2x})/(a_1 + a_2) \\ p_2 &= (a_2 A_1 \dot{\theta}_{1x} - a_1 A_2 \dot{\theta}_{2x})/(a_1 + a_2)^2 \\ p_3 &= (a_2 A_1 \dot{\theta}_{1x} - a_1 A_2 \dot{\theta}_{2x})/\Delta \end{aligned}$$

$$P_4 = (a_2^2 A_1 \dot{\theta}_{1x} + a_1^2 A_2 \dot{\theta}_{2x}) / (a_1 + a_2) \Delta$$

$$\alpha = a_1 / (a_1 + a_2)$$

$$a_i = C_i^* - K^2, \quad i = 1, 2$$

and

$$\Delta = C_1^* C_2^* - K^2.$$

It should be emphasized that the variables  $\eta$  and  $\zeta$  indicate the relative misalignment between the body 1 and 2 y-axes and z-axes respectively. The variables Y and Z are analogous to translational coordinates of the center of mass of the two body system.

With the use of equations (3-2) and (3-3), the forcing term of the equations of motion (3-5) reduces to

$$\begin{bmatrix} \ell \zeta / (a_1 + a_2) \\ - \ell \eta / (a_1 + a_2) \\ - [(a_1 + a_2) L_{Ay} - a_1 \zeta \ell] / \Delta \\ - [(a_1 + a_2) L_{Az} + a_1 \eta \ell] / \Delta \end{bmatrix} \quad (3-6)$$

if the despin torque is applied in body 1 and

$$\begin{bmatrix} - \ell \zeta / (a_1 + a_2) \\ - \ell \eta / (a_1 + a_2) \\ - [(a_1 + a_2) L_{Ay} + a_2 \zeta \ell] / \Delta \\ - [(a_1 + a_2) L_{Az} + a_2 \eta \ell] / \Delta \end{bmatrix} \quad (3-7)$$

if the despin torque is applied in body 2. It is easily seen that when there is no despin torque, the forcing term reduces to

$$\begin{bmatrix} 0 \\ 0 \\ -(a_1 + a_2) L_{Ay}/\Delta \\ -(a_1 + a_2) L_{Az}/\Delta \end{bmatrix}$$

With equations (3-6) and (3-7), equation (3-5) can now be written as

$$\begin{bmatrix} \ddot{Y} \\ \ddot{Z} \\ \ddot{\eta} \\ \ddot{\zeta} \end{bmatrix} + \begin{bmatrix} 0 & p_1 & 0 & -p_2 \\ -p_1 & 0 & p_2 & 0 \\ 0 & -p_3 & 0 & p_4 \\ p_3 & 0 & -p_4 & 0 \end{bmatrix} \begin{bmatrix} \dot{Y} \\ \dot{Z} \\ \dot{\eta} \\ \dot{\zeta} \end{bmatrix} + \begin{bmatrix} 0 & 0 & 0 & -g \\ 0 & 0 & g & 0 \\ 0 & 0 & 0 & -f_i \\ 0 & 0 & f_i & 0 \end{bmatrix} \begin{bmatrix} Y \\ Z \\ \eta \\ \zeta \end{bmatrix} = \begin{bmatrix} 0 \\ 0 \\ -h L_{Ay} \\ -h L_{Az} \end{bmatrix} \quad (3-8)$$

with

$$f_i = (-1)^{i+1} \frac{a_i}{\Delta} \ell$$

$$g = \ell / (a_1 + a_2)$$

and

$$h = (a_1 + a_2) / \Delta$$

where the subscript

$i = 1$ , when the despin torque is applied in body 1

$i = 2$ , when the despin torque is applied in body 2 .

Consequently, the state variable canonical form of the linearized model in terms of phase variable format is, in general, given by

$$\begin{bmatrix} \dot{\eta} \\ \dot{\zeta} \\ \ddot{Y} \\ \ddot{Z} \\ \ddot{\eta} \\ \ddot{\zeta} \end{bmatrix} = \begin{bmatrix} 0 & 0 & 0 & 0 & 1 & 0 \\ 0 & 0 & 0 & 0 & 0 & 1 \\ 0 & g & 0 & -p_1 & 0 & p_2 \\ -g & 0 & p_1 & 0 & -p_2 & 0 \\ 0 & f_i & 0 & p_3 & 0 & -p_4 \\ -f_i & 0 & -p_3 & 0 & p_4 & 0 \end{bmatrix} \begin{bmatrix} \eta \\ \zeta \\ \dot{Y} \\ \dot{Z} \\ \dot{\eta} \\ \dot{\zeta} \end{bmatrix} + \begin{bmatrix} 0 & 0 \\ 0 & 0 \\ 0 & 0 \\ 0 & 0 \\ -h & 0 \\ 0 & -h \end{bmatrix} \begin{bmatrix} L_{Ay} \\ L_{Az} \end{bmatrix} \quad (3-9)$$



This equation coupled with the following x-directional equations of motion (for rotation about the x-axes of the bodies),

$$A_1 \ddot{\theta}_{1x} = L_{1x} = \ell$$

and

$$A_2 \ddot{\theta}_{2x} = -L_{2x} = -\ell,$$

(3-10)

forms a complete description of the linear model.

## Section IV

## A-1 CONTROL OPTION - BODY 1 HAS THREE AXIS ATTITUDE CONTROL

## 4.1 REDUCED EQUATIONS OF MOTION

For the A-1 control option, whereby body 1 has ideal three axis attitude control, the constraint equations

$$\dot{\theta}_{1x} = \dot{\theta}_{1y} = \dot{\theta}_{1z} = 0$$

can be used to further simplify the two-body equations of motion. Applying these conditions to equation (3-1) results in a set of four equations

$$\begin{aligned} -K \ddot{\theta}_{2y} &= \hat{L}_{1y} \\ -K \ddot{\theta}_{2z} &= \hat{L}_{1z} \\ C_2^* \ddot{\theta}_{2y} + A_2 \dot{\theta}_{2x} \dot{\theta}_{2z} &= -\hat{L}_{2y} \\ C_2^* \ddot{\theta}_{2z} - A_2 \dot{\theta}_{2x} \dot{\theta}_{2y} &= -\hat{L}_{2z} \end{aligned} \quad (4-1)$$

the last two of which are sufficient for studying the behavior of body 2 relative to body 1. With the use of equations (3-2) and (3-3), then

$$\begin{aligned} \hat{L}_{2y} &= L_{Ay} - \ell\theta_{2z} + \ell\theta_{1z} \\ \hat{L}_{2z} &= L_{Az} + \ell\theta_{2y} - \ell\theta_{1y} \end{aligned}$$

if the despin torque is applied in body 1 and

$$\begin{aligned} \hat{L}_{2y} &= L_{Ay} \\ \hat{L}_{2z} &= L_{Az} \end{aligned}$$

if the despin torque is applied in body 2. Since  $\theta_{1y}$  and  $\theta_{1z}$  are both constants, then there is no loss of generality if they are assumed equal to zero. Therefore, the last two equations of (4-1) can be rewritten as

$$\begin{bmatrix} \ddot{\theta}_{2y} \\ \ddot{\theta}_{2z} \end{bmatrix} + \begin{bmatrix} 0 & -\hat{\omega} \\ \hat{\omega} & 0 \end{bmatrix} \begin{bmatrix} \dot{\theta}_{2y} \\ \dot{\theta}_{2z} \end{bmatrix} + \begin{bmatrix} 0 & -q_i \\ q_i & 0 \end{bmatrix} \begin{bmatrix} \theta_{2y} \\ \theta_{2z} \end{bmatrix} = \begin{bmatrix} -L_{Ay}/C_2^* \\ -L_{Az}/C_2^* \end{bmatrix}$$

or in state variable canonical form

$$\begin{bmatrix} \dot{\theta}_{2y} \\ \dot{\theta}_{2z} \\ \ddot{\theta}_{2y} \\ \ddot{\theta}_{2z} \end{bmatrix} = \begin{bmatrix} 0 & 0 & 1 & 0 \\ 0 & 0 & 0 & 1 \\ 0 & \hat{\ell}_i & 0 & -\hat{\omega} \\ -\hat{\ell}_i & 0 & \hat{\omega} & 0 \end{bmatrix} \begin{bmatrix} \theta_{2y} \\ \theta_{2z} \\ \dot{\theta}_{2y} \\ \dot{\theta}_{2z} \end{bmatrix} + \begin{bmatrix} 0 & 0 \\ 0 & 0 \\ -1/C_2^* & 0 \\ 0 & -1/C_2^* \end{bmatrix} \begin{bmatrix} L_{Ay} \\ L_{Az} \end{bmatrix}$$

where

$$\hat{\omega} = \frac{A_2}{C_2^*} \dot{\theta}_{2x} \quad ,$$

$$\hat{\ell}_1 = \frac{\ell}{C_2^*} \quad (\text{when the despin torque is applied to body 1})$$

and

$$\hat{\ell}_2 = 0 \quad (\text{when the despin torque is applied to body 2}).$$

With the above assumption that  $\dot{\theta}_{1y} = \theta_{1y} = \dot{\theta}_{2y} = \theta_{2y} = 0$ , then the alignment torque given by equation (3-4) reduces to

$$L_{Ay} = k \theta_{2y} + \lambda \dot{\theta}_{2y}$$

$$L_{Az} = k \theta_{2z} + \lambda \dot{\theta}_{2z}$$

and the state variable canonical form can be still further reduced to

$$\begin{bmatrix} \dot{\theta}_{2y} \\ \dot{\theta}_{2z} \\ \ddot{\theta}_{2y} \\ \ddot{\theta}_{2z} \end{bmatrix} = \begin{bmatrix} 0 & 0 & 1 & 0 \\ 0 & 0 & 0 & 1 \\ -\hat{k} & \hat{\ell}_i & -\hat{\lambda} & -\hat{\omega} \\ -\hat{\ell}_i & -\hat{k} & \hat{\omega} & -\hat{\lambda} \end{bmatrix} \begin{bmatrix} \theta_{2y} \\ \theta_{2z} \\ \dot{\theta}_{2y} \\ \dot{\theta}_{2z} \end{bmatrix} \quad (4-2)$$

where

$$\hat{k} = \frac{k}{C_2^*}$$

and

$$\hat{\lambda} = \frac{\lambda}{C_2^*} .$$

## 4.2 LINEAR MODEL OPEN-LOOP BEHAVIOR, DECOMPOSITION, AND INTERPRETATION

In this subsection, the open loop behavior (that is, without the spring/damper alignment torque) of the linear model will be investigated first without a despin torque (in subsection 4.2.1) and secondly with a despin torque (in subsection 4.4.2). In both cases, body 1 is assumed to have ideal 3-axis attitude control. Numerical calculations will be based on the nominal model as presented in subsection 2.3.

### 4.2.1 Open-Loop Behavior Without the Despin Torque (A-1, L-1)

For the case of the linear model with neither an alignment nor a despin torque,  $k = \lambda = l = 0$  and equation (4-2) reduces to

$$\begin{bmatrix} \dot{\theta}_{2y} \\ \dot{\theta}_{2z} \\ \ddot{\theta}_{2y} \\ \ddot{\theta}_{2z} \end{bmatrix} = \begin{bmatrix} 0 & 0 & 1 & 0 \\ 0 & 0 & 0 & 1 \\ 0 & 0 & 0 & -b \\ 0 & 0 & b & 0 \end{bmatrix} \begin{bmatrix} \theta_{2y} \\ \theta_{2z} \\ \dot{\theta}_{2y} \\ \dot{\theta}_{2z} \end{bmatrix}$$

where

$$b = \frac{A_2}{C_2^*} \omega_o$$

$$\omega_o = \dot{\theta}_{2x0} \text{ (a constant).}$$

Computation shows that there are four open-loop poles on the imaginary axis:

$$P_1 = 0$$

$$P_2 = 0$$

$$P_3 = 0.2003 j$$

$$P_4 = -0.2003 j$$

As was mentioned in subsection 2.1, no definite conclusion about the total system stability can be made by Liapunov's first method if the linear model cannot be shown to be unstable or asymptotically stable. The appearance of the multiple zero poles, however, further motivates the study at hand. For if both of the zero poles appear in the  $\theta_{2y}$  or  $\theta_{2z}$  process, the system would be linearly unstable and hence, nonlinearly unstable. If they do not, then the linear analysis cannot reveal the overall stability.

By rearranging the order of state variables in equation (4-2), the state-space description becomes

$$\begin{bmatrix} \dot{\theta}_{2y} \\ \ddot{\theta}_{2y} \\ \theta_{2z} \\ \dot{\theta}_{2z} \end{bmatrix} = \begin{bmatrix} 0 & 1 & 0 & | & 0 \\ 0 & 0 & b & | & 0 \\ 0 & -b & 0 & | & 0 \\ 0 & 0 & 1 & | & 0 \end{bmatrix} \begin{bmatrix} \theta_{2y} \\ \dot{\theta}_{2y} \\ \theta_{2z} \\ \dot{\theta}_{2z} \end{bmatrix}$$

with the output variable

$$\theta_{2y} = \begin{bmatrix} 1 & 0 & 0 & | & 0 \end{bmatrix} \begin{bmatrix} \theta_{2y} \\ \dot{\theta}_{2y} \\ \theta_{2z} \\ \dot{\theta}_{2z} \end{bmatrix}$$

From the partitioned matrix, it is readily seen that the  $\theta_{2z}$  process is unobservable (references 1, 3) from the  $\theta_{2y}$  process and that the  $\theta_{2y}$  process can be described by a state space of dimension three. That is, the subsystem

$$\begin{bmatrix} \dot{\theta}_{2y} \\ \ddot{\theta}_{2y} \\ \theta_{2z} \end{bmatrix} = \begin{bmatrix} 0 & 1 & 0 \\ 0 & 0 & b \\ 0 & -b & 0 \end{bmatrix} \begin{bmatrix} \theta_{2y} \\ \dot{\theta}_{2y} \\ \theta_{2z} \end{bmatrix}$$

and

$$\theta_{2y} = \begin{bmatrix} 1 & 0 & 0 \end{bmatrix} \begin{bmatrix} \theta_{2y} \\ \dot{\theta}_{2y} \\ \dot{\theta}_{2z} \end{bmatrix}$$

can be separated from the original system. With this reduced state-space description, which can be shown to be completely observable, it can be seen that there are three modes in the  $\theta_{2y}$  process, namely

$$\begin{aligned} P_1 &= 0 \\ P_2 &= bj \\ P_3 &= -bj \end{aligned}$$

which implies only linear stability. Since similar results can be shown for the  $\theta_{2z}$  process, no immediate conclusions about overall stability can be made based on a linear analysis.

Due to the special structure of the system, however, a study of the  $\dot{\theta}_{2y}$  and  $\dot{\theta}_{2z}$  process is warranted. Again by rearranging the order of state variables, the state-space description becomes

$$\begin{bmatrix} \ddot{\theta}_{2y} \\ \ddot{\theta}_{2z} \\ \dot{\theta}_{2y} \\ \dot{\theta}_{2z} \end{bmatrix} = \begin{bmatrix} 0 & b & 0 & 0 \\ -b & 0 & 0 & 0 \\ 1 & 0 & 0 & 0 \\ 0 & 1 & 0 & 0 \end{bmatrix} \begin{bmatrix} \dot{\theta}_{2y} \\ \dot{\theta}_{2z} \\ \theta_{2y} \\ \theta_{2z} \end{bmatrix}$$

with the output

$$\begin{bmatrix} \dot{\theta}_{2y} \\ \dot{\theta}_{2z} \end{bmatrix} = \begin{bmatrix} 1 & 0 & 0 & 0 \\ 0 & 1 & 0 & 0 \end{bmatrix} \begin{bmatrix} \dot{\theta}_{2y} \\ \dot{\theta}_{2z} \\ \theta_{2y} \\ \theta_{2z} \end{bmatrix}$$

After separating this equation into the subsystems

$$\begin{bmatrix} \ddot{\theta}_{2y} \\ \ddot{\theta}_{2z} \end{bmatrix} = \begin{bmatrix} 0 & b \\ -b & 0 \end{bmatrix} \begin{bmatrix} \dot{\theta}_{2y} \\ \dot{\theta}_{2z} \end{bmatrix}$$

and

$$\begin{bmatrix} \dot{\theta}_{2y} \\ \dot{\theta}_{2z} \end{bmatrix} = \begin{bmatrix} 1 & 0 \\ 0 & 1 \end{bmatrix} \begin{bmatrix} \dot{\theta}_{2y} \\ \dot{\theta}_{2z} \end{bmatrix},$$

it is readily seen that the  $\dot{\theta}_{2y}$  and  $\dot{\theta}_{2z}$  processes are governed by two modes:  $bj$  and  $-bj$ , which means sustained oscillation in the precession rates.

#### 4.2.2 Open-Loop Behavior With the Despin Torque

The effect on the stability of a single rigid body upon application of a despin torque has been discussed in subsection 3.3.2.2 of reference 4. The case for the above linear model without an alignment torque but with a constant despin torque is discussed in the following.

Considering first, the x-directional equation of motion, equation (3-10)

$$A_2 \ddot{\theta}_{2x} = -L_{2x} = -\ell, \quad \dot{\theta}_{2x} \neq 0$$

then

$$\ddot{\theta}_{2x} = -\frac{\ell}{A_2}$$

and

$$\dot{\theta}_{2x} = -\frac{\ell}{A_2} t + \omega_0, \quad 0 \leq t \leq t_D$$

where the despin time,  $t_D$ , is given by

$$t_D = \frac{A_2 \omega_0}{\ell}$$

and  $\omega_0$  is the value of  $\dot{\theta}_{2x}$  at  $t = 0$ . The appearance of  $\dot{\theta}_{2x}$  in the coefficients of the y and Z directional equations of motion (equation 4-2) makes the system time-varying. Although the trajectory of the system poles cannot, in general, be used as a criterion of stability for time-varying systems (references 5, 6),

some sufficient-existent type perturbational results exist (reference 7) which can provide one with some kind of feeling about the system stability behavior, as long as the time-varying perturbation terms are either small or slowly varying.

The unperturbed model is obtained from equation (4-2) by freezing the time at a particular value. If the despin torque is assumed to be applied to body 1 and the time is frozen at  $t=0$ , then the unperturbed model is given as

$$\begin{bmatrix} \dot{\theta}_{2y} \\ \dot{\theta}_{2z} \\ \ddot{\theta}_{2y} \\ \ddot{\theta}_{2z} \end{bmatrix} = \begin{bmatrix} 0 & 0 & 1 & 0 \\ 0 & 0 & 0 & 1 \\ 0 & \hat{l}_1 & 0 & b \\ -\hat{l}_1 & 0 & -b & 0 \end{bmatrix} \begin{bmatrix} \theta_{2y} \\ \theta_{2z} \\ \dot{\theta}_{2y} \\ \dot{\theta}_{2z} \end{bmatrix}$$

where

$$b = \frac{A_2}{C_2^*} \omega_o$$

and the time-varying perturbation comes from

$$\Delta \dot{\theta}_{2x} = \dot{\theta}_{2x} - \omega_o$$

which has a time constant of  $0.63 t_D$  for a given despin time,  $t_D$ .

Numerical calculation shows that, for a given despin time, the time constant of the unperturbed system is about equal to  $t_D$ . Compared with the system time constant, the perturbation variation is not too slow, but is not too fast either. Consequently, the pole location analysis should still be able to reveal some information about the transient behavior of the system. Numerical results obtained for the unperturbed model frozen at  $t = 0$  and  $t = t_D/2$  are presented in Table 4-1. The appearance of the positive poles suggests an unstable tendency in the time behavior. For the case when the despin torque is applied, body 2 instability is also indicated. This is because  $\dot{\theta}_{2x}$  will eventually go to zero and according to equation (4-2) and the analysis presented in subsection 4.2.1, multiple zero poles would appear in the  $\theta_{2y}$  or the  $\theta_{2z}$  process.



Table 4-1. OPEN-LOOP POLES/WITH DESPIN TORQUE

$t_D$ (sec)	POLES ( $t = 0$ )	POLES ( $t = t_D/2$ )
20	-0.04551 ± 0.2101j +0.04551 ± 0.009858j	-0.06251 ± 0.1301 +0.06251 ± 0.03002j
60	-0.01644 ± 0.2016j +0.01644 ± 0.001341j	-0.02887 ± 0.1078j +0.02887 ± 0.007728j
120	-0.008304 ± 0.2001j +0.008304 ± 0.0003436j	-0.01588 ± 0.1026j +0.01588 ± 0.002459j
180	-0.005547 ± 0.2004j +0.005547 ± 0.0001534j	-0.01085 ± 0.1013j +0.01085 ± 0.001163j

**4.3 LINEAR MODEL CLOSED-LOOP BEHAVIOR**

In this subsection, the closed-loop behavior (that is, with the spring/damper alignment torque) of the linear model will be investigated first without a despin torque (in subsection 4.3.1) and secondly with a despin torque (in subsection 4.3.2). In both cases, body 1 is assumed to have ideal 3-axis attitude control. Numerical calculations will be based on the nominal model as presented in subsection 2.3.

**4.3.1 Closed-Loop Behavior Without the Despin Torque**

For the case of the linear model with the alignment torque but without the despin torque,  $\ell = 0$  and equation (4-2) reduces to

$$\begin{bmatrix} \dot{\theta}_{2y} \\ \dot{\theta}_{2z} \\ \ddot{\theta}_{2y} \\ \ddot{\theta}_{2z} \end{bmatrix} = \begin{bmatrix} 0 & 0 & 1 & 0 \\ 0 & 0 & 0 & 1 \\ -\hat{k} & 0 & -\hat{\lambda} & -b \\ 0 & -\hat{k} & b & -\hat{\lambda} \end{bmatrix} \begin{bmatrix} \theta_{2y} \\ \theta_{2z} \\ \dot{\theta}_{2y} \\ \dot{\theta}_{2z} \end{bmatrix}$$

where

$$b = \frac{A_2}{C_2^*} \omega_o$$

and  $\omega_0$  is a constant.

It can be shown analytically that, for any spring/damper combination ( $k > 0$ ,  $\lambda > 0$ ), the linearized model is always asymptotically stable, that is, the spring/damper compensated system is absolutely stable which implies that the nonlinear model is also absolutely asymptotically stable.

For damped harmonic motion, the critically-damped case is generally the most efficient for stabilization purposes. The following sample design is based on a simplified model for which  $\theta_{2y}$  and  $\theta_{2z}$  are decoupled. Choosing

$$k = 0.01 C_2^* = 216.64 \text{ Kg-m}^2/\text{rad-sec}^2$$

$$\lambda = 0.2 C_2^* = 4332.8 \text{ Kg-m}^2/\text{rad-sec}$$

then a pole-configuration for the real system is obtained as

$$P_1 = -0.1786 + 0.2275j$$

$$P_2 = -0.1786 - 0.2275j$$

$$P_3 = -0.0213 + 0.0271j$$

$$P_4 = -0.0213 - 0.0271j$$

As a preliminary analysis, the time constant and the oscillation period for both the first and second conjugate pairs,  $(P_1, P_2)$  and  $(P_3, P_4)$  respectively, are given in Table 4-2 for  $P = -\sigma \pm \omega j$ .

Table 4-2. CLOSED-LOOP TIME CONSTANTS AND PERIODS/WITHOUT DESPIN TORQUE

	TIME CONSTANT $\tau = 1/\sigma$ (sec)	OSCILLATION PERIOD $\tau = 2\pi/\omega$ (sec)
$P_1, P_2$	$\approx 5.6$	$\approx 27.6$
$P_3, P_4$	$\approx 46.8$	$\approx 231.6$

From Table 4-2, it can be seen that an initial offset would damp out relatively fast. A more detailed analysis, along with discussion of system structure, zero configuration, and general design rule will be presented in subsection 4.4.

#### 4.3.2 Closed-Loop Behavior with the Despin Torque

The case of the linear model with both the alignment and the despin torque is represented by equation (4-2), whereby the system coefficient matrix is time varying. For  $t > t_D$ , the system reduces to a model similar to that discussed in subsection 4.3.1, which was shown to be asymptotically stable. Based on a steady-state stability theorem (reference 6) then, the asymptotic stability of the perturbed closed-loop system with despin torque is guaranteed.

#### 4.4 SOME STRUCTURAL PROPERTIES, PERFORMANCE EVALUATION, AND GENERAL DESIGN GUIDELINE

Owing to the existence of various combinations of two body parameters (mass, inertia, and joint vector), a specific set of design values based on a nominal model may not be very helpful. However, it is believed that regardless of the specific configuration of interest, the structure and some other properties of the compensated nominal model should be preserved. Hence, it is of both theoretical and practical interest, to study system structure from which a general design rule may be obtained.

Basic structural properties are controllability, observability, and coupling/interaction. It is easy to see that the closed-loop model, with either  $\theta_{2y}$ ,  $\theta_{2z}$ ,  $\dot{\theta}_{2y}$  or  $\dot{\theta}_{2z}$  as a single output, is both (input-state) controllable and (state-output) observable, as long as  $k > 0$  and  $\lambda > 0$  (so that no pole-zero cancellation can occur). In other words, each of  $\theta_{2y}$ ,  $\theta_{2z}$ ,  $\dot{\theta}_{2y}$ , or  $\dot{\theta}_{2z}$  contain all of the four modes.

A further analysis of time-behavior requires the knowledge of zero-locations which in turn determines the importance of each pole. However, it is known that for a multi-input system, the zeros of the transfer function matrix are functions of both subsystem interaction and state variable feedback. For this underlying simple structure, it can be shown that the state output resolvent matrix  $(C(\underline{IS} - \underline{A})^{-1})$  of reference 2) with  $\theta_{2y}$  and  $\theta_{2z}$  as output, has the form

$$\begin{bmatrix} \theta_{2y} \\ \theta_{2z} \end{bmatrix} = \begin{bmatrix} \frac{(s + \hat{\lambda})(s^2 + \hat{\lambda}s + \hat{k}) + b^2s}{\Delta_c} & \frac{s^2 + \hat{\lambda}s + \hat{k}}{\Delta_c} & \frac{-b\hat{k}}{\Delta_c} & \frac{-bs}{\Delta_c} \\ \frac{b\hat{k}}{\Delta_c} & \frac{bs}{\Delta_c} & \frac{(s + \hat{\lambda})(s^2 + \hat{\lambda}s + \hat{k}) + b^2s}{\Delta_c} & \frac{s^2 + \hat{\lambda}s + \hat{k}}{\Delta_c} \end{bmatrix} \begin{bmatrix} \dot{\theta}_{2y0} \\ \dot{\theta}_{2z0} \\ \theta_{2y0} \\ \theta_{2z0} \end{bmatrix}$$

where

S - Laplace transform variable

$\Delta_c$  - characteristic polynomial of the coupled model

and  $\theta_{2y0}$ ,  $\dot{\theta}_{2y0}$ ,  $\theta_{2z0}$ , and  $\dot{\theta}_{2z0}$  are the initial states in the state-space.

For the nominal model (see subsection 2.3), the coupling coefficient, b, has a value of 0.20032. Without a more sophisticated measure of system interaction (reference 8), it can readily be seen that the  $\theta_{2y}$  and  $\theta_{2z}$  processes are weakly coupled if b is small compared with  $\hat{k}$  and  $\hat{\lambda}$ . An extreme case is given by  $b = 0$ , whereby the  $\theta_{2y}$  and  $\theta_{2z}$  processes are decoupled and hence unobservable from each other. In addition to the disappearance of those coupling terms in the resolvent matrix, pole-zero cancellations of the roots of  $s^2 + \hat{\lambda}s + \hat{k}$  occur. These cancellations make each process,  $\theta_{2y}$  or  $\theta_{2z}$ , contain only two modes, that is, the other two modes corresponding to say the  $\theta_{2z}$  process have no weight in the dynamics of the  $\theta_{2y}$  process. When  $b \neq 0$ , but the subsystems are only weakly coupled, then the above situation should not change too much. This means that the roots of the characteristic polynomial of the coupled system are close to the roots of the characteristic polynomial of the decoupled system,  $(s^2 + \hat{\lambda}s + \hat{k})^2$ , and that only two modes are dominant in each subprocess.

A root locus plot for the coupled system where  $\hat{k}$  is held constant and  $\hat{\lambda}$  is varied, and where  $\hat{\lambda}$  is held fixed and  $\hat{k}$  is varied is shown in Figure 4-1. Numerical data for this figure are given in Table 4-3.

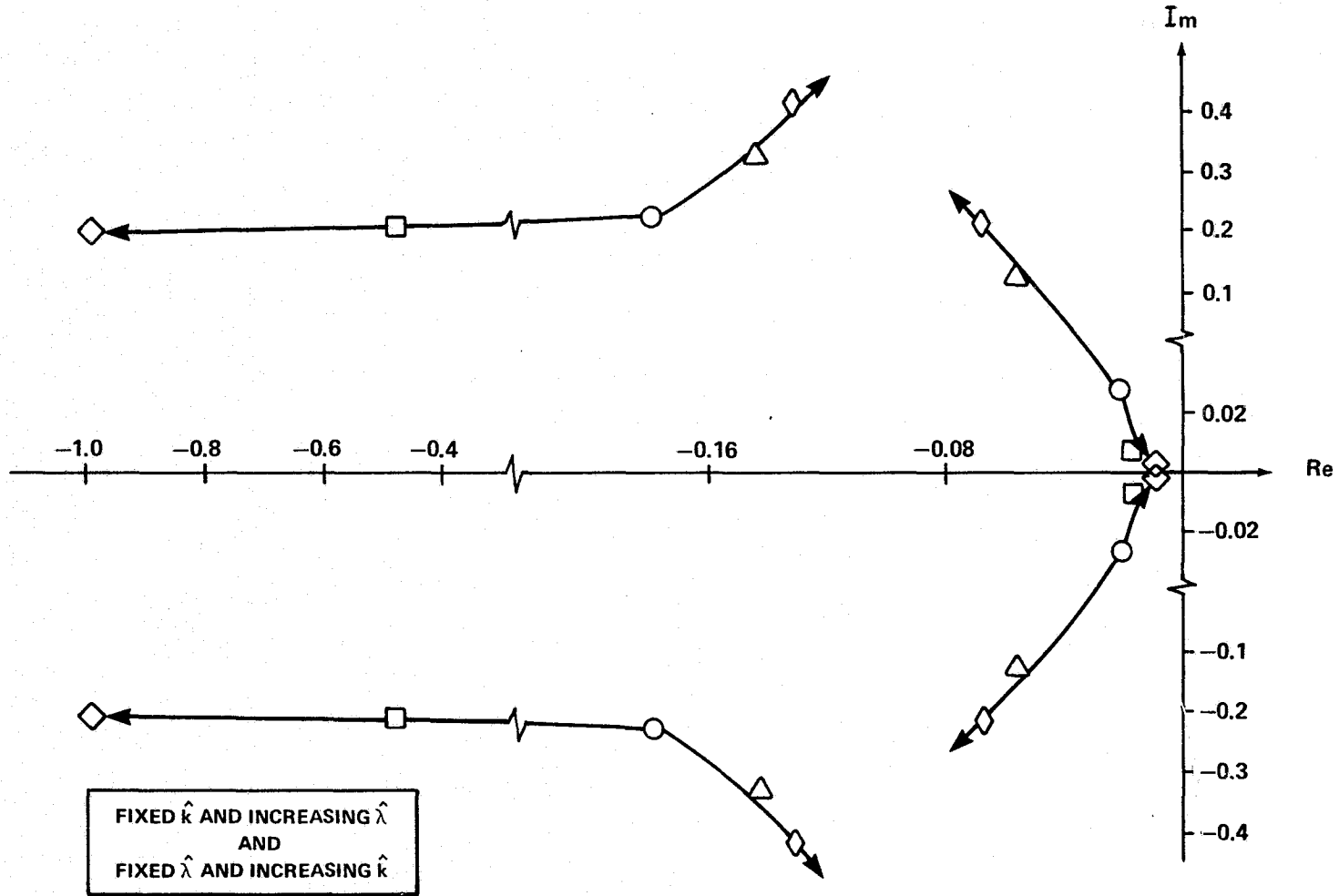


Figure 4-1. COUPLED SYSTEM ROOT LOCUS DIAGRAM

Table 4-3. NUMERICAL DATA FOR FIGURE 4-1

PLOT SYMBOL	$\hat{k}$	$\hat{\lambda}$	DATA
◇	0.01	1.0	-0.0096 ± 0.0019j -0.9903 ± 0.2023j
□	0.01	0.5	-0.0174 ± 0.0075j -0.4825 ± 0.2078j
○	0.01	0.2	-0.0213 ± 0.0271j -0.1786 ± 0.2275j
△	0.05	0.2	-0.0560 ± 0.1277j -0.1439 ± 0.3281j
◇	0.10	0.2	-0.0684 ± 0.2176j -0.1315 ± 0.4180j

From the above discussion and graphic illustration, the following general guideline can be summarized:

- Subprocess interaction has the effect of introducing oscillation in the mean time separating the two conjugate pairs.
- Subprocess interaction is decreased as  $b$  becomes smaller, particularly when  $\omega_0$  is small or  $\hat{k}$  and  $\hat{\lambda}$  are large.
- In general, interaction is mild because the root-locus shows a good command of system pole-location through spring/damper feedback.
- The decoupled model, being a good approximation when interaction is weak, is suggested for use in design purposes.
- Because of the oscillation effect introduced by coupling, slight overdamping is recommended. For instance, design values of  $\hat{k} = 0.01$  and  $\hat{\lambda} = 0.5$  may be good. However, excessive damping should be avoided, otherwise the slow transient conjugate pair would be dominant.

## Section V

A-2/A-3 CONTROL OPTION -- BODY 1  
HAS X-AXIS ONLY OR NO ATTITUDE CONTROL

The cases to be considered in this section are less restrictive than those discussed in Section IV. Namely, body 1 is assumed to have only x-directional attitude control (A-2) or no attitude control at all (A-3). It should be noted that x-axis only attitude control is implied by the condition  $\dot{\theta}_{1x} = 0$ . The state variable canonical form of the linearized model to be used in this section is given by equation (3-9).

## 5.1 LINEAR MODEL OPEN-LOOP BEHAVIOR, DECOMPOSITION, AND INTERPRETATION

In this subsection, the open-loop behavior (that is, without the spring/damper alignment torque) of the linear model will be investigated first without a despin torque (in subsection 5.1.1) and secondly with a despin torque (in subsection 5.1.2) for both the A-2 and the A-3 control options. Numerical calculations will be based on the nominal model as presented in subsection 2.3.

## 5.1.1 Open-Loop Behavior Without the Despin Torque

It can be readily seen from equation (3-8) that the Y and Z processes are unobservable from the  $\eta$  and  $\zeta$  processes. Therefore, the state-space dimension can be reduced to six, and such a six-dimensional realization can be shown to be a minimal realization if  $\eta$  and  $\zeta$  are considered as output. Furthermore, if  $\eta$  and  $\zeta$  are considered as output separately, it can be shown that a five-dimensional realization would be sufficient and is completely observable. On this basis, the state-space description for the  $\eta$ -process for when neither the alignment nor the despin torque are active can be written as

$$\begin{bmatrix} \dot{\eta} \\ \ddots \\ \dot{Y} \\ \ddots \\ \dot{Z} \\ \ddots \\ \dot{\eta} \\ \ddots \\ \dot{\zeta} \end{bmatrix} = \begin{bmatrix} 0 & 0 & 0 & 1 & 0 \\ 0 & 0 & -p_1 & 0 & p_2 \\ 0 & p_1 & 0 & -p_2 & 0 \\ 0 & 0 & p_3 & 0 & -p_4 \\ 0 & -p_3 & 0 & p_4 & 0 \end{bmatrix} \begin{bmatrix} \eta \\ \dot{Y} \\ \dot{Z} \\ \dot{\eta} \\ \dot{\zeta} \end{bmatrix}$$

with the output

$$\eta = \begin{bmatrix} 1 & 0 & 0 & 0 & 0 \end{bmatrix} \begin{bmatrix} \eta \\ \dot{\eta} \\ \dot{\zeta} \\ \eta \\ \zeta \end{bmatrix} .$$

It should be noted that a similar form holds for the  $\zeta$ -process.

For the A-2 control option, the nominal model indicates there are five modes in the dynamics of either  $\eta$  or  $\zeta$ , namely

$$\begin{aligned} P_1 &= P_2 = P_3 = 0 \\ P_4 &= 0.2767j \\ P_5 &= -0.2767j. \end{aligned}$$

It can be shown analytically that when body 1 has only x-axis attitude control ( $\dot{\theta}_{1x} = 0$ ), there are, in general, always three zero poles, since the system matrix has a 3-dimensional null space. Because of the multiple zero poles and the observability of the system, the  $\eta$  or  $\zeta$  process is open-loop linearly unstable and therefore nonlinearly unstable. It can also be shown that the  $\eta$  and  $\zeta$  process is not observable from the  $\dot{\eta}$  and  $\dot{\zeta}$  process and therefore a four-dimensional realization exists for the  $\dot{\eta}$  and  $\dot{\zeta}$  process. That is to say that the  $\dot{\eta}$  and  $\dot{\zeta}$  process can be separated from the  $\eta$  and  $\zeta$  process and contains four modes. The imaginary poles generally imply sustained oscillation in the relative precession rates whereas, the multiple poles reveal, in this case, the nonlinear instability of the  $\dot{\eta}$  and  $\dot{\zeta}$  process. Since the total energy is finite, a limit cycle type instability would be expected.

For the A-3 control option, body 1 is assumed to be initialized with a perfectly matching angular velocity as compared to body 2. In so doing, the basic structure of the problem will remain the same as that for the A-2 control option. Based on the nominal model, the numerical values of the five modes in  $\eta$  or  $\zeta$  become



$$P_1 = 0$$

$$P_2 = 0.2810j$$

$$P_3 = -0.2810j$$

$$P_4 = 0.01063j$$

$$P_5 = -0.01063j$$

Since there is only one zero pole along with two imaginary conjugate pairs, the linear analysis fails to predict overall stability.

### 5.1.2 Open-Loop Behavior with the Despin Torque

The case of the linear model without the alignment torque but with a constant despin torque is discussed here relative to the A-2 and A-3 control modes. For x-directional attitude control of body 1 (A-2), the despin dynamics is similar to that discussed in subsection 4.2.2 for the A-1 control mode, that is,  $\dot{\theta}_{2x}$  should decrease linearly to zero. The same arguments as presented in subsection 4.2.2 are applicable here, that is, plausibility is based on perturbational results. Numerical results obtained for the unperturbed model frozen at  $t = 0$  and  $t_D/2$  for the case when the despin torque is applied to body 1 are presented in Table 5-1. Similarly, when the despin torque is applied to body 2, there is a complex conjugate pair of poles in the right-half plane for each case, which suggests an unstable tendency relative to misalignment.

For the A-3 control option, body 1 is again assumed to be initialized with an angular velocity perfectly matching that of body 2, implying that an x-directional attitude control of body 1 is required to design the system. This reduces the problem to essentially that just discussed for the A-2 control mode. More generally, however, if the initial angular speed of body 1,  $\omega_1$ , is different from  $\omega_0$  (the value of  $\dot{\theta}_{2x}$  at  $t = 0$ ), then the following despin time could be separated, that is,

$$t_D = A^* \frac{\Delta\omega}{\ell}$$

where  $A^* = A_1 A_2 / (A_1 + A_2)$  and  $\Delta\omega = \omega_0 - \omega_1$ .

Table 5-1. OPEN-LOOP POLES/WITH DESPIN TORQUE

$t_D(\text{sec})$	POLES ( $t = 0$ )	POLES ( $t = t_D/2$ )
30	0,0	0,0
	$-0.04082 \pm 0.2826j$	$-0.06296 \pm 0.1627j$
	$+0.04082 \pm 0.005897j$	$+0.06296 \pm 0.02436j$
60	0,0	0,0
	$-0.02104 \pm 0.2783j$	$-0.03743 \pm 0.1478j$
	$+0.02104 \pm 0.001590j$	$+0.03743 \pm 0.009479j$
90	0,0	0,0
	$-0.01411 \pm 0.2774j$	$-0.02650 \pm 0.1432j$
	$+0.01411 \pm 0.0007181j$	$+0.02650 \pm 0.004901j$
120	0,0	0,0
	$-0.01061 \pm 0.2771j$	$-0.02041 \pm 0.1413j$
	$+0.01061 \pm 0.0004062j$	$+0.02041 \pm 0.002948j$

**5.2 LINEAR MODEL CLOSED-LOOP BEHAVIOR**

In this subsection, the closed-loop behavior (that is, with the spring/damper alignment torque) of the linear model will be investigated first without a despin torque (in subsection 5.2.1) and secondly with a despin torque (in subsection 5.2.2). In both cases, body 1 is assumed to have x-axis only attitude control (that is,  $\dot{\theta}_{1x} = 0$ ). Numerical calculations will be based on the nominal model as presented in subsection 2.3.

**5.2.1 Closed-Loop Behavior Without the Despin Torque**

It can readily be shown that, without the despin torque and using the alignment torque as defined by equation (3-4), the state variable canonical form of the linearized model can be expressed as

$$\begin{bmatrix} \dot{\eta} \\ \dot{\zeta} \\ \ddots \\ \dot{Y} \\ \ddots \\ Z \\ \ddots \\ \dot{\eta} \\ \ddots \\ \dot{\zeta} \end{bmatrix} = \begin{bmatrix} 0 & 0 & 0 & 0 & 1 & 0 \\ 0 & 0 & 0 & 0 & 0 & 1 \\ 0 & 0 & 0 & -p_1 & 0 & p_2 \\ 0 & 0 & p_1 & 0 & -p_2 & 0 \\ -\bar{k} & 0 & 0 & p_3 & -\bar{\lambda} & -p_4 \\ 0 & -\bar{k} & -p_3 & 0 & p_4 & -\bar{\lambda} \end{bmatrix} \begin{bmatrix} \eta \\ \zeta \\ \dot{Y} \\ \dot{Z} \\ \dot{\eta} \\ \dot{\zeta} \end{bmatrix}$$

where  $\bar{k} = hk$  and  $\bar{\lambda} = h\lambda$ . This system is composed of two coupled subsystems, namely the  $\eta$  and  $\zeta$  process and the  $\dot{Y}$  and  $\dot{Z}$  process. Only the  $\eta$  and  $\zeta$  process can be directly controlled by the spring/damper alignment torque. A further study of the system reveals that the  $\dot{Y}$  and  $\dot{Z}$  subsystem has associated with it two pure imaginary poles which will introduce some oscillation throughout the system. Therefore, a pair of conjugate poles are expected to exist which cannot be moved very far from the imaginary axis. However, it is not unreasonable to assume that these two slow-transient poles will have little effect on  $\eta$  or  $\zeta$  if the coupling is weak. An analytic proof of the absolute stability of this linear model would probably be difficult to obtain because of the system order. In Section VI, a Liapunov-type approach involving the original nonlinear system will be presented.

In the following sample design, the spring and damper constants are chosen to make the isolated  $\eta$  and  $\zeta$  process critically damped. Choosing  $k$  and  $\lambda$  as

$$k = \bar{k}/h = 0.01/h = 85.601 \text{ kg-m}^2/\text{rad-sec}^2$$

$$\lambda = \bar{\lambda}/h = .2/h = 1712.0 \text{ kg-m}^2/\text{rad-sec}$$

results in the following pole-configuration:

$$P_1 = -0.1718 + 0.2917j$$

$$P_2 = -0.1718 - 0.2917j$$

$$P_3 = -0.02604 + 0.03537j$$

$$P_4 = -0.02604 - 0.03537j$$

$$P_5 = -0.002088 + 0.02032j$$

$$P_6 = -0.002088 - 0.02032j$$

It is readily recognized that the first two pairs are attributed primarily to the  $\eta$  and  $\zeta$  subsystem and the third pair is due primarily to the  $\dot{Y}$  and  $\dot{Z}$  subsystem. The first pair represents fast-transient modes, whereas the second pair is slower, having a time constant of 38.4 seconds and a modal oscillation period of 180 seconds, which implies a pretty good damping effect. The third pair corresponds to very slow transient modes which have a time constant of 478.7 seconds and an oscillation period of 390.3 seconds.

Although it is reasonable to expect the third pair to have little importance in  $\eta/\eta_0$ ,  $\eta/\zeta_0$ ,  $\eta/\dot{\eta}_0$ ,  $\eta/\dot{\zeta}_0$ , etc., it may have some persistent effect in the impulse response of  $\eta/\dot{Y}_0$ ,  $\eta/\dot{Z}_0$ , etc. A detailed analysis would require a pole-zero map and the understanding of the system structure, both of which will be presented in subsection 5.3.

It might also be expected that the effect of the slow transient pair on  $\eta/\dot{Y}_0$ , etc. could be reduced by an increase in the energy storage and dissipation capability, that is, by increasing  $\bar{k}$  and  $\bar{\lambda}$ . Choosing  $\bar{k} = 1$  and  $\bar{\lambda} = 2$  gives  $k = 8360.1$  and  $\lambda = 17120$ , resulting in the following pole-configuration:

$$\begin{aligned} P_1 &= -1.33505 + 0.49056j \\ P_2 &= -1.33505 - 0.49056j \\ P_3 &= -0.664929 + 0.243993j \\ P_4 &= -0.664929 - 0.243993j \\ P_5 &= -0.0000133094 + 0.030170j \\ P_6 &= -0.0000133094 - 0.030170j \end{aligned}$$

It is interesting to note that the third pair moves even closer to the imaginary axis. This phenomenon will be self-evident after the discussion of interaction in subsection 5.3. From a pole-configuration standpoint, there does not appear to be any improvement relative to an increase in  $\bar{k}$  and  $\bar{\lambda}$ . However, a more detailed pole-zero and time response study to be presented in subsection 5.3 will show that the latter of the above two designs is indeed much better than the first.

### 5.2.2 Closed-Loop Behavior With the Despin Torque

The case of the linear model with both the alignment and the despin torque is represented by equation (3-9) whereby the system coefficient matrix is time varying. For  $t > t_D$ , the system reduces to a model similar to that discussed in subsection 5.2.1, whereby asymptotic stability of the perturbed closed-loop system with despin would be preserved (based on a steady-state stability theorem (reference 6)).

5.3 SOME STRUCTURAL PROPERTIES, PERFORMANCE EVALUATION, AND GENERAL DESIGN GUIDELINE

It can be readily shown that the spring/damper compensated system for any  $k > 0$  and  $\lambda > 0$  is completely observable with the six-dimensional state-space representation and the scalar output of  $\eta$ ,  $\zeta$ ,  $\dot{\eta}$  or  $\dot{\zeta}$ . Therefore, all of the six modes will appear in  $\eta$  or  $\zeta$ . It was shown in subsection 5.2 that there is one conjugate pair corresponding to slow-transient modes and for which a root-locus analysis showed that they cannot be moved far away from the imaginary axis. Since we are interested in the dynamics of  $\eta$  and  $\zeta$  as opposed to that of  $\dot{Y}$  or  $\dot{Z}$ , the zero locations and hence the residues of those modes in the resolvent matrix of  $\eta$  and  $\zeta$  are essential in determining the importance of those slow-transient modes in the dynamics of  $\eta$  and  $\zeta$ . Prior to giving any numerical results, a general discussion of the system interaction will be presented, which should be useful when considering the variant models.

It was mentioned in subsection 5.2 that the overall system can be viewed as consisting of two subsystems coupled together where only one of these subsystems could have external inputs (see Figure 5-1). Mesarović (reference 8) labels this form as a V-canonical structure.

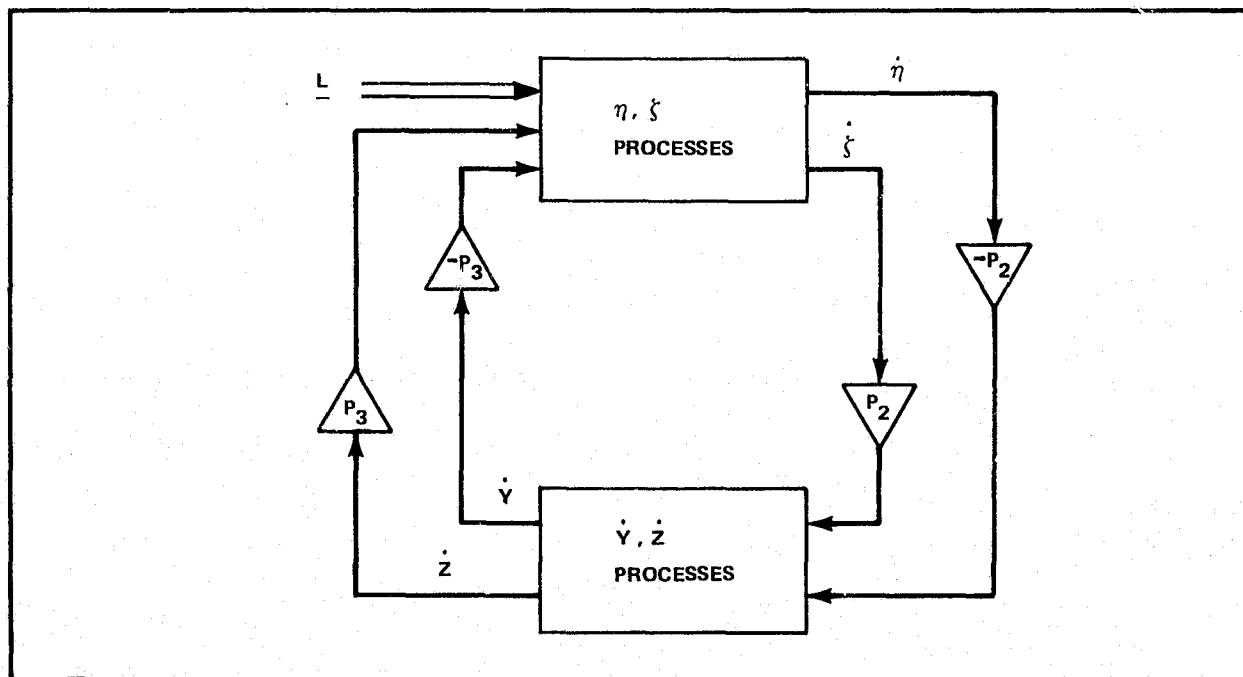


Figure 5-1. V-CANONICAL STRUCTURE MODEL

These two subsystems can be denoted by

$$\begin{bmatrix} \eta \\ \zeta \end{bmatrix} = [H_0(S)] \begin{bmatrix} \eta_o \\ \zeta_o \\ \dot{\eta}_o \\ \dot{\zeta}_o \end{bmatrix}$$

and

$$\begin{bmatrix} \eta \\ \zeta \end{bmatrix} = [H_1(S)] \begin{bmatrix} \dot{Y}_o \\ \dot{Z}_o \end{bmatrix}$$

where

$[H_0(S)]$  - resolvent matrix from the  $\eta_o, \zeta_o, \dot{\eta}_o$  and  $\dot{\zeta}_o$  subspace to  $\eta$  and  $\zeta$ .

$[H_1(S)]$  - resolvent matrix from the  $\dot{Y}_o$  and  $\dot{Z}_o$  subspace to  $\eta$  and  $\zeta$ .

It is interesting to note that the subsystems are coupled through the parameters  $p_2$  and  $p_3$ . If  $p_3$  is zero, then the  $\dot{Y}$  and  $\dot{Z}$  processes would be unobservable from the  $\eta$  and  $\zeta$  processes and hence the two open-loop poles of  $\dot{Y}$  and  $\dot{Z}$  would be cancelled by two zeros in  $[H_0(S)]$ . In general, there are two zeros in  $[H_0(S)]$  which are zeros having the generic form of

$$(s^2 + p_1^2) + f(p_3, S)$$

where  $f(p_3, S)$  is a rational function in the Laplace Transform variable  $S$  which is continuous in  $p_3$  and equals zero if  $p_3 = 0$ . Also, the two open-loop poles of  $\dot{Y}$  and  $\dot{Z}$  are given by  $+p_1j$  and  $-p_1j$ . If the interaction is weak or  $p_3$  is small, there will be two zeros in  $[H_0(S)]$  which are close to these two slow-transient poles. Consequently, they will have little influence on  $[H_0(S)]$  and the behavior of  $[H_0(S)]$  should be similar to that discussed in subsection 4.3.1 for the closed-loop system without the despin torque and body 1 with 3-axis ideal attitude control.

On the other hand, if  $p_2 = 0$ , the resolvent matrix  $[H_1(S)]$  can be written as

$$[H_1(S)] = \begin{bmatrix} \frac{s^2 + \bar{\lambda}s + \bar{k}}{\Delta_o} & \frac{-p_4 s}{\Delta_o} \\ \frac{p_4 s}{\Delta_o} & \frac{s^2 + \bar{\lambda}s + \bar{k}}{\Delta_o} \end{bmatrix} \begin{bmatrix} \frac{p_1 p_3}{s^2 + p_1^2} & \frac{p_3 s}{s^2 + p_1^2} \\ \frac{p_3 s}{s^2 + p_1^2} & \frac{-p_1 p_3}{s^2 + p_1^2} \end{bmatrix}$$

$$= \begin{bmatrix} \frac{p_3 [p_1 (s^2 + \bar{\lambda}s + \bar{k}) - p_4 s^2]}{\Delta_o (s^2 + p_1^2)} & \frac{p_3 s [s^2 + \bar{\lambda}s + \bar{k} + p_1 p_4]}{\Delta_o (s^2 + p_1^2)} \\ \frac{p_3 s [s^2 + \bar{\lambda}s + \bar{k} + p_1 p_4]}{\Delta_o (s^2 + p_1^2)} & \frac{-p_3 [p_1 (s^2 + \bar{\lambda}s + \bar{k}) - p_4 s^2]}{\Delta_o (s^2 + p_1^2)} \end{bmatrix}$$

where  $\Delta_o$  is the open-loop characteristic polynomial of the  $\eta$  and  $\zeta$  processes. The structure of this configuration is expressed as shown in Figure 5-2.

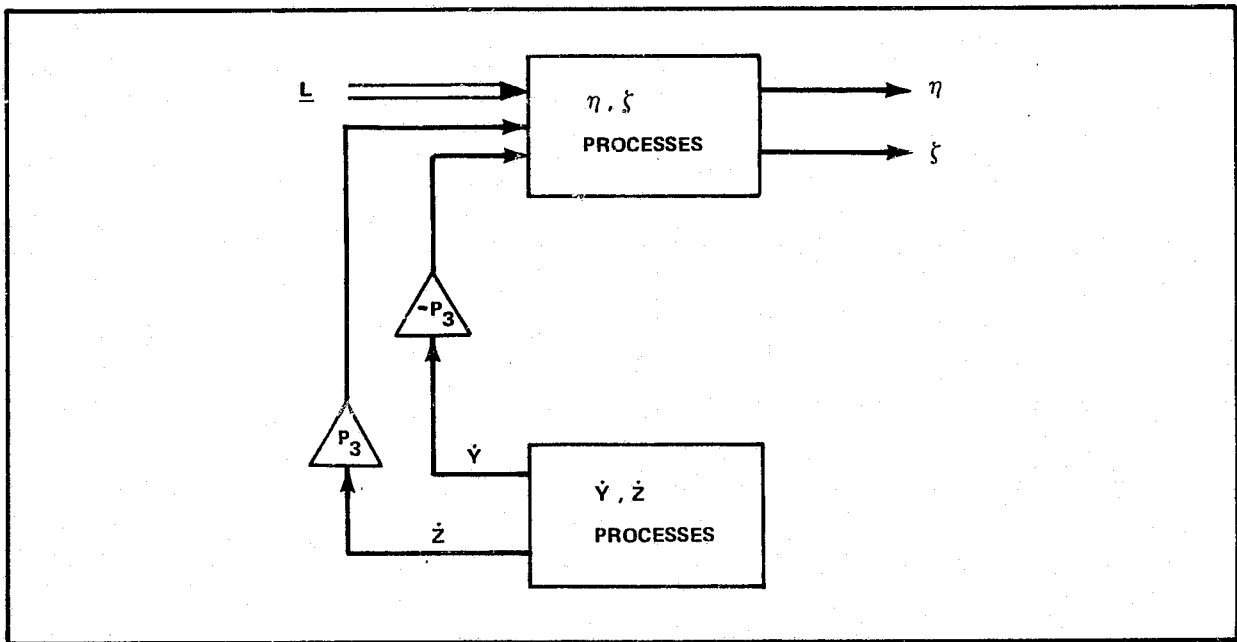


Figure 5-2. SIMPLIFIED STRUCTURE I

Considering the six poles according to their order as discussed in subsection 5.2.1 (that is, the fast-transient pair as the first pair, the intermediate-transient pair as the second pair, and the slow-transient pair as the third pair), then the  $H_1$  transformation for  $p_2 = 0$  indicates that both the second and third pairs will be important. Even when  $p_2 \neq 0$ , the situation should not change too much if the interaction is weak or intermediate. Also, as  $p_2$  gets smaller, the slow-transient pair will move closer to the imaginary axis and as  $p_3$  gets smaller, the slow-transient pair will be less involved in the  $\eta$  and  $\zeta$  dynamics. These observations are summarized in Table 5-2 where

the important pole pairs were determined by the residue of the respective transfer function. Analogous conclusions can also be made for the dynamics of  $\zeta$ .

Table 5-2. IMPORTANT POLE-PAIRS

TRANSFER FUNCTION	IMPORTANT POLE-PAIRS
$\eta/\eta_0$	2 <sup>nd</sup> pair
$\eta/\zeta_0$	2 <sup>nd</sup> pair
$\eta/\dot{\eta}_0$	1 <sup>st</sup> and 2 <sup>nd</sup> pair
$\eta/\dot{\zeta}_0$	1 <sup>st</sup> and 2 <sup>nd</sup> pair
$\eta/\dot{Y}_0$	2 <sup>nd</sup> and 3 <sup>rd</sup> pair
$\eta/\dot{Z}_0$	2 <sup>nd</sup> and 3 <sup>rd</sup> pair

Several points relative to the above discussion should be mentioned at this time. First, the above conclusions are more plausible when interaction becomes weaker (when  $p_3$  becomes smaller or  $\bar{k}$  and  $\bar{\lambda}$  become larger as compared with  $p_3$ ). Secondly, the slow-transient modes are important only in the  $\eta/\dot{Y}_0$  and  $\eta/\dot{Z}_0$  transfers where  $\dot{Y}_0$  and  $\dot{Z}_0$  are given relative to  $\dot{\theta}_{1y0}$ ,  $\dot{\theta}_{2y0}$ ,  $\dot{\theta}_{1z0}$ , and  $\dot{\theta}_{2z0}$  which are assumed fairly small. Thirdly, the important pole-pairs listed for a particular transfer function were determined through a comparison with that transfer function only and the importance of each pole-pair relative to all the transfer functions listed in Table 5-1 was not considered. Finally, the amplitudes for each pole-pair in every impulse response were not determined. However, it is expected that the amplitudes of the impulse responses  $\eta/\dot{Y}_0$  and  $\eta/\dot{Z}_0$  would be reduced when interaction becomes smaller.

The coupling factors  $p_1$ ,  $p_2$ ,  $p_3$ , and  $p_4$  of the nominal model when body 1 has ideal x-directional attitude control (the A-2 control mode) are numerically given in Table 5-3. It is interesting to note that the  $\dot{Z}$ ,  $\dot{Y}$  to  $\eta$ ,  $\zeta$  coupling factor  $p_3$  is pretty large if  $\bar{k}$  and  $\bar{\lambda}$  are chosen as  $\bar{k} = 0.1$  and  $\bar{\lambda} = 0.2$ , so that a larger influence from  $\dot{Z}_0$ ,  $\dot{Y}_0$  to  $\eta$ ,  $\zeta$  is expected. In Table 5-4, numerical data is given for the poles, zeros, and gain associated with the appropriate element of the resolvent matrix for each of the indicated transfer functions. In each case, the spring and damping were chosen as  $\bar{k} = 0.01$  and  $\bar{\lambda} = 0.2$ . In addition, any number having an absolute value less than  $10^{-4}$  was



truncated. It is of interest to note that these numerical results agree quite well with the summary of general characteristics.

Table 5-3. COUPLING FACTORS

COUPLING	FACTORS
$\dot{Y}$ to $\dot{Z}$	$p_1 = 0.03039$
$\zeta, n$ to $\dot{Y}, \dot{Z}$	$p_2 = -0.02118$
$\dot{Y}, \dot{Z}$ to $\zeta, n$	$p_3 = -0.03534$
$n$ to $\zeta$	$p_4 = 0.02463$

Table 5-4. POLES, ZEROS, AND GAIN OF THE RESOLVENT MATRIX

TRANSFER	POLES	ZEROS	GAIN
$\frac{\eta}{\eta_0}$	-0.1718 ± 0.2917j -0.02604 ± 0.03537j -0.002088 ± 0.02032j	-0.1772 ± 0.2792j -0.02924 -0.008110 ± 0.02261j	1
$\frac{\eta}{\zeta_0}$	-0.1718 ± 0.2917j -0.02604 ± 0.03537j -0.002088 ± 0.02032j	0, 0	0.002463
$\frac{\dot{\eta}}{\dot{\eta}_0}$	-0.1718 ± 0.2917j -0.02604 ± 0.03537j -0.002088 ± 0.02032j	-0.09769 ± 0.08614j -0.002309 ± 0.02322j	1
$\frac{\dot{\eta}}{\dot{\zeta}_0}$	-0.1718 ± 0.2917j -0.02604 ± 0.03537j -0.002088 ± 0.02032j	0 0, 0	-0.2463
$\frac{\dot{\eta}}{\dot{Y}_0}$	-0.1718 ± 0.2917j -0.02604 ± 0.03537j -0.002088 ± 0.02032j	-0.01098 ± 0.03126j	-0.09780
$\frac{\dot{\eta}}{\dot{Z}_0}$	-0.1718 ± 0.2917j -0.02604 ± 0.03537j -0.002088 ± 0.02032j	-0.1 -0.1 0	-0.3534

In general, the time response of a given transfer function can be expressed as

$$r(t) = G \left[ \sum_{i=1}^k R_i e^{-\lambda_i t} + 2 \sum_{i=1}^m C_i e^{-\lambda_i t} \cos(\omega_i t + \delta_i) \right]$$

where

- $R_i$  - the residue corresponding to the real mode,  $-\lambda_i$
- $2C_i$  - the residue corresponding to the complex modes,  $-\lambda_i \pm \omega_i j$
- $\delta_i$  - the phase shift
- $G$  - the gain

In Table 5-5 numerical data are given for  $\bar{k} = 0.01$  and  $\bar{\lambda} = 0.2$  summarizing the residues and phase shifts for each of the modes considered.

Table 5-5. RESIDUES AND PHASE SHIFTS

TRANSFER	POLES (PAIRS)	2GC <sub>i</sub> (WEIGHT)	PHASE SHIFT
$n/n_0$	1 <sup>st</sup> /2 <sup>nd</sup> /3 <sup>rd</sup>	0.08055/0.74146/0.25925	-0.9288/-0.2455/-0.4596
$n/\zeta_0$	1 <sup>st</sup> /2 <sup>nd</sup> /3 <sup>rd</sup>	0.08043/0.74041/0.25898	-5.6412/-1.8153/-1.1111
$n/\dot{n}_0$	1 <sup>st</sup> /2 <sup>nd</sup> /3 <sup>rd</sup>	2.7276/3.257/0.5297	-1.9673/-1.1806/-1.9279
$n/\dot{\zeta}_0$	1 <sup>st</sup> /2 <sup>nd</sup> /3 <sup>rd</sup>	-2.7276/-3.257/-0.52968	-3.5381/0.39014/2.7843
$n/\dot{Y}_0$	1 <sup>st</sup> /2 <sup>nd</sup> /3 <sup>rd</sup>	-3.0814/-16.2723/-18.2039	-5.6905/-1.5577/-1.7234
$n/\dot{Z}_0$	1 <sup>st</sup> /2 <sup>nd</sup> /3 <sup>rd</sup>	-3.0814/-16.2719/-18.2036	-4.1197/-3.1285/-0.15268

Numerical calculation shows that the time impulse response of  $|n/Z_0|$  has maximum peak values of 12.4, 13.23, 9.44, and 6.83 radians at times of 40, 155, 310, and 465 seconds respectively. Similar peak values also appear in the  $|n/\dot{Y}_0|$  time response. Consequently, initial wobble may have a large effect on the relative misalignment. The nominal value of 0.1 rad/sec for  $\dot{\theta}_{2x0}$  is almost the largest possible spin-rate. For a mild wobble, a value of 0.01 rad/sec for  $\dot{\theta}_{2y0}$  or  $\dot{\theta}_{2z0}$  would be reasonable, resulting in a damped sinusoidal oscillation in misalignment with an amplitude of about 3.159 degrees during the first 200 seconds. This oscillation, having an initial period of about

250 seconds which would increase with time, has its amplitude decreasing exponentially with a time constant of about 500 seconds. Although the situation for this kind of initial wobble is not too serious, an undesired situation may occur if either  $\dot{\theta}_{2y_0}$  or  $\dot{\theta}_{2z_0}$  has a value of 0.05 rad/sec since this would result in an initial modal oscillation amplitude of 15.79 degrees.

Some attention then should be paid to the behavior of the  $\eta/\dot{Y}_0$  and  $\eta/\dot{Z}_0$  transfers. It has been observed that the two slow-transient modes are unavoidable regardless of the values chosen for the spring and damper coefficients. So at best, one can only try to reduce the amplitudes of  $\eta/\dot{Y}_0$  and  $\eta/\dot{Z}_0$ . At this preliminary design stage, it is desirable to develop a formula which can be used to estimate the oscillation amplitude of  $\eta/\dot{Y}_0$  or  $\eta/\dot{Z}_0$  for a given value of  $\bar{k}$  and  $\bar{\lambda}$ . Based on the simplified model presented below, such a formula is developed, the accuracy of which improves as the subsystem interaction becomes weaker.

Suppose that the  $\eta$  and  $\zeta$  processes were decoupled and would not influence the  $\dot{Y}$  and  $\dot{Z}$  processes, but the  $\dot{Y}$  and  $\dot{Z}$  processes could influence the  $\eta$  and  $\zeta$  processes. Graphically, this situation is illustrated in Figure 5-3. Due to the structure of the  $\dot{Y}$  and  $\dot{Z}$  subsystem, the resulting  $\dot{Y}$  and  $\dot{Z}$  processes are sinusoidal functions with a frequency of  $p_1/2\pi$ , that is,

$$\begin{aligned}\dot{Y}(t) &= \dot{Y}_0 \cos p_1 t + \dot{Z}_0 \sin p_1 t \\ \dot{Z}(t) &= -\dot{Y}_0 \sin p_1 t + \dot{Z}_0 \cos p_1 t.\end{aligned}$$

Assuming that the spring/damper feedback loops are closed for the  $\eta$  and  $\zeta$  processes, the above problem is readily recognized as a problem of forced oscillation with damping, which can be described by

$$\ddot{x} + \bar{\lambda}\dot{x} + \bar{k}x = a \cos \omega t$$

and the particular (steady state) solution to this equation can be written as

$$x_2(t) = A \cos (\omega t - \phi)$$

where the amplitude  $A$  and phase  $\phi$  are given by

$$A = \frac{a}{\sqrt{(\bar{k} - \omega^2)^2 + \bar{\lambda}^2 \omega^2}}$$

and

$$\phi = \tan^{-1} \left( \frac{\bar{\lambda} \omega}{\bar{k} - \omega^2} \right)$$

Consequently, it is readily seen that for  $\dot{Y}_0 = 0$ , an estimate of the amplitude of the slow-transient modes in the impulse response  $\eta/\dot{Z}_0$  can be given by

$$\hat{A} = \frac{|p_3|}{\sqrt{(\bar{k} - p_1^2)^2 + \bar{\lambda}^2 p_1^2}} \tag{5-1}$$

From this formula, it is easy to see how the amplitude will be reduced as  $\bar{k}$  and  $\bar{\lambda}$  increase, a phenomenon which has been predicted from a subsystem interaction point of view.

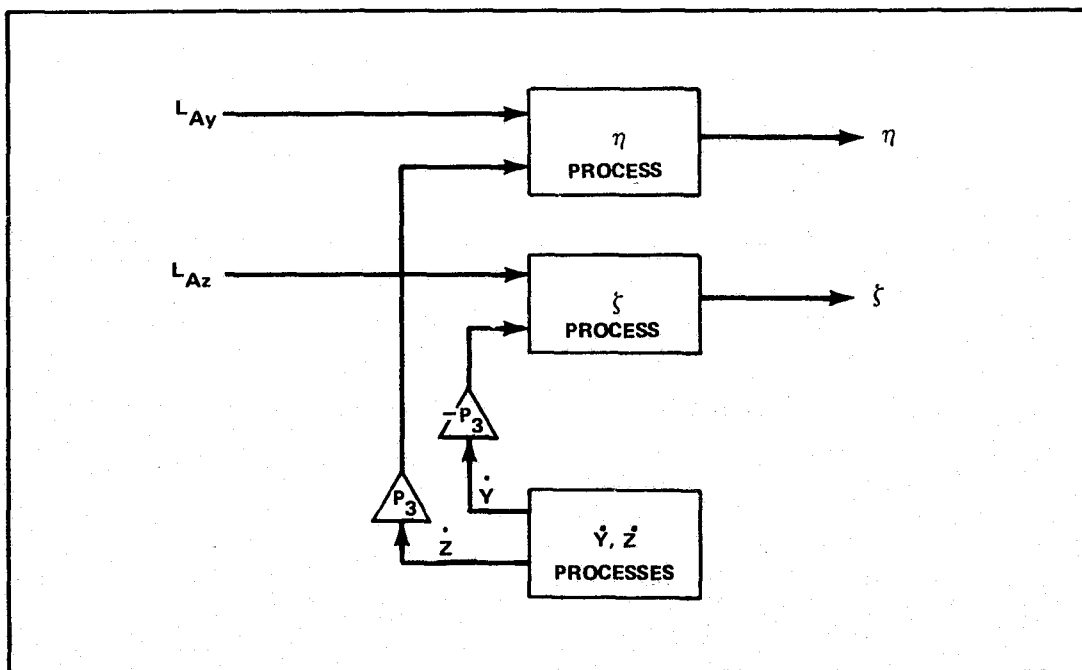


Figure 5-3. SIMPLIFIED STRUCTURE II

A comparison of the estimated amplitude and the calculated "true" amplitude is presented in Table 5-6. From this table it is immediately apparent that as  $\bar{k}$  and  $\bar{\lambda}$  increase, the accuracy of the estimate provided by the formula increases. In addition, the data indicates that by using more control effort ( $\bar{k}$  and  $\bar{\lambda}$ ), the overall system performance is maintained while reducing the amplitude of the  $\eta/\dot{Z}_0$  and  $\eta/\dot{Y}_0$  transfers.

Table 5-6. A COMPARISON OF ESTIMATED AND ACTUAL AMPLITUDES

CONTROL EFFORT	ESTIMATED AMPLITUDE, $\hat{A}$	TRUE AMPLITUDE FOR THE 3 <sup>rd</sup> PAIR IN $\eta/\dot{Z}_0$	TIME CONSTANT FOR THE 3 <sup>rd</sup> PAIR (SEC)	OVERALL AMPLITUDE FOR IMPULSE RESPONSE $\eta/\dot{Z}_0$
$\bar{k} = 0.01$ $\bar{\lambda} = 0.2$	32.35	18.20	478.76	13.23
$\bar{k} = 0.36$ $\bar{\lambda} = 1.2$	0.9791	0.9414	17361	0.9348
$\bar{k} = 0.64$ $\bar{\lambda} = 1.6$	0.5514	0.5391	39308	0.5367
$\bar{k} = 1$ $\bar{\lambda} = 2$	0.3530	0.3463	75187	0.3450

The root locus diagram shown in Figure 5-4 shows the general trend of the system-pole movement. It should be noted that the third pair of poles cannot be moved further to the left from the imaginary axis by increasing the damping ratio. Although a slight movement to the left was observed for smaller values of  $\bar{k}$  and  $\bar{\lambda}$ , decreasing the values of  $\bar{k}$  and  $\bar{\lambda}$  would also result in undesirably larger amplitudes of the slow-transient modes in the  $\eta/\dot{Z}_0$  or  $\eta/\dot{Y}_0$  transfer. In general then, one should not pay much attention to the location of these two poles. Instead, the formula should be used to choose suitable magnitudes of  $\bar{k}$  and  $\bar{\lambda}$  which will give satisfactory performance for the first and the second pairs and yet make the amplitude of the third pair in the  $\eta/\dot{Z}_0$  and  $\eta/\dot{Y}_0$  transfers smaller than a maximum tolerable value.

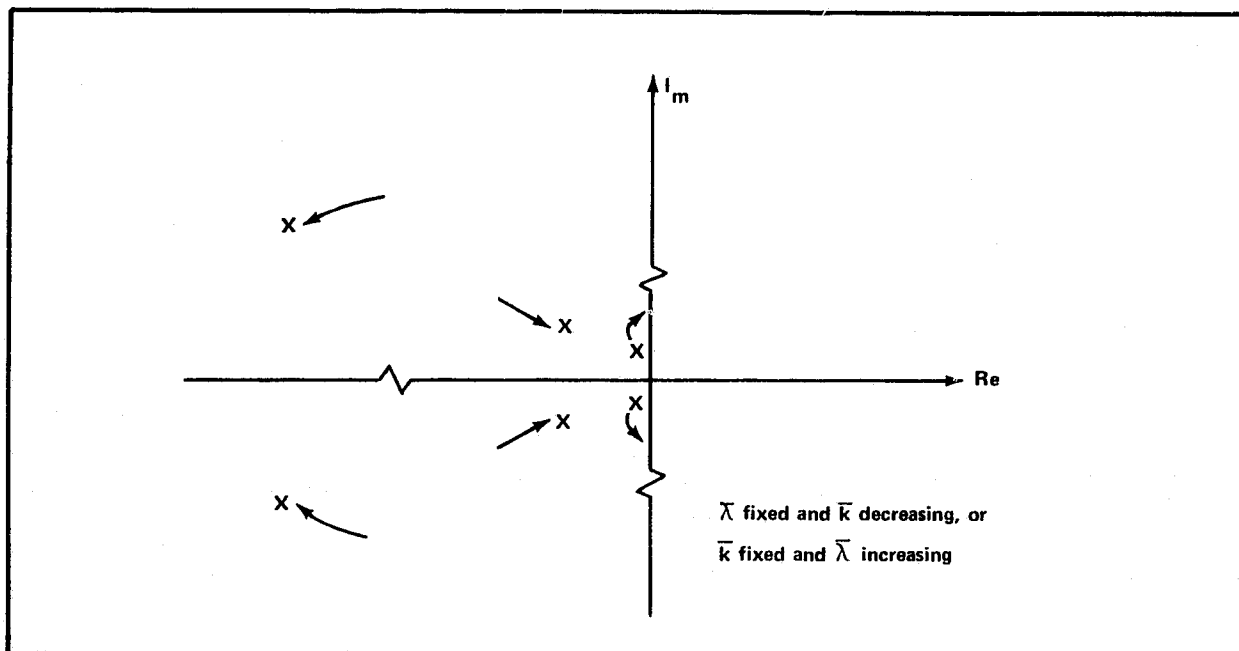


Figure 5-4. ROOT LOCUS DIAGRAM

At this point, one can state some generalizations and a design guideline for the spring/damper compensated coupled spinning system:

1. The influence of the  $\dot{Y}$ ,  $\dot{Z}$  subsystem on the  $\eta$  and  $\zeta$  processes cannot be efficiently controlled by spring/damper feedback. In particular, two slow-transient modes which are primarily attributed to the  $\dot{Y}$ ,  $\dot{Z}$  subsystem will have considerable importance in the  $\eta/\dot{Z}_0$ ,  $\eta/\dot{Z}_0$ ,  $\zeta/\dot{Y}_0$ , and  $\zeta/\dot{Y}_0$  transfers. The importance of these slow-transient modes will be reduced as the  $\dot{Y}$ ,  $\dot{Z}$  to  $\eta$ ,  $\zeta$  interaction becomes weaker. There are two ways to reduce the interaction. One is to reduce  $p_3$  bilinearly by adjusting the body 1 x-directional spin-rate (to be discussed in subsection 5.4). Another one is to increase the magnitudes of  $\bar{k}$  and  $\bar{\lambda}$ . A formula which gives an approximate relation between  $\bar{k}$ ,  $\bar{\lambda}$ , and the amplitude of the slow-transient modes was given by equation (5-1).
2. The coupling of the  $\dot{Y}$ ,  $\dot{Z}$  and  $\eta$ ,  $\zeta$  processes has the effect of introducing some oscillation in the mean time and tends to separate the first pair from the second.
3. Based on items 1 and 2, a stabilization design procedure can be outlined in the following three steps:
  - a) Use of equation (5-1) to choose the magnitudes of  $\bar{k}$  and  $\bar{\lambda}$  which would meet a maximum tolerable limit on the amplitude of the  $\eta/\dot{Z}_0$  transfer.

- b) Use a decoupled/non-interacting model to choose the damping ratio, etc., to control the behavior of  $\eta/\eta_0$ ,  $\eta/\zeta_0$ ,  $\eta/\dot{\eta}_0$ ,  $\eta/\dot{\zeta}_0$ ,  $\zeta/\eta_0$ ,  $\zeta/\zeta_0$ ,  $\zeta/\dot{\eta}_0$ , and  $\zeta/\dot{\zeta}_0$ . Critical or slightly over damped is recommended.
- c) Run a root-locus and time-response analysis, etc., to confirm that this preliminary design is satisfactory.

#### 5.4 EFFECTS OF INITIAL ANGULAR SPEED MATCHING

In a number of instances in the foregoing discussion, ideal x-directional attitude control on body 1 was assumed. If in addition, pre-spin docking is assumed, then some effects on the misalignment dynamics might be expected, because the strength of system interaction could be changed. Imposing the initial condition of perfect angular speed matching, that is,  $\dot{\theta}_{1x0} = \dot{\theta}_{2x0} = \omega_0$ , on the definitions of the coupling factors  $p_2$  and  $p_3$  given in subsection 3.3 as

$$p_2 = (a_2 A_1 \dot{\theta}_{1x} - a_1 A_2 \dot{\theta}_{2x}) / (a_1 + a_2)^2$$

$$p_3 = (a_2 A_1 \dot{\theta}_{1x} - a_1 A_2 \dot{\theta}_{2x}) / \Delta$$

results in

$$p_2 = \omega_0 (a_2 A_1 - a_1 A_2) / (a_1 + a_2)^2$$

$$p_3 = \omega_0 (a_2 A_1 - a_1 A_2) / \Delta.$$

If  $p_2$  and  $p_3$  are denoted by  $\bar{p}_2$  and  $\bar{p}_3$  for the case when body 1 has x-directional attitude control and  $\hat{p}_2$  and  $\hat{p}_3$  for when body 1 has no attitude control, then for the initial condition of perfect angular speed matching, the conditions

$$|\hat{p}_2| < |\bar{p}_2| \quad \text{and} \quad |\hat{p}_3| < |\bar{p}_3|$$

hold as long as  $a_2 A_1 < 2a_1 A_2$ . The implication here is that the  $\eta$ ,  $\zeta$  and  $\dot{Y}$ ,  $\dot{Z}$  interaction would be weakened, thereby providing better overall system performance. Based on the nominal model,  $a_2 A_1$  and  $a_1 A_2$  are equal to 364,139,780.7 and 4,319,741,524 respectively and the above inequality is seen to be satisfied.

The above discussion suggests that for any given body 2 (satellite) spin rate ( $\omega_0$ ), there always exists a body 1 (tug) matching speed ( $\omega_1^*$ ) given by

$$\omega_1^* = \frac{a_1 A_2}{a_2 A_1} \omega_o$$

such that the  $\eta$ ,  $\zeta$  and  $\dot{Y}$ ,  $\dot{Z}$  processes become noninteracting. Therefore, the two slow-transient modes will not affect the dynamics of  $\eta$  and  $\zeta$ . It is interesting to note that with this ideal matching speed, the model reduces to a form similar to that found for the case where body 1 has ideal 3-axis attitude control. Therefore, the same performance of relative misalignment as for the case when body 1 has full attitude control can be achieved by prespinning body 1 to the ideal matching speed. However, this kind of bilinear control is not of practical interest, at least for this nominal model, because of the large value of the ratio,  $a_1 A_2 / a_2 A_1$ .



## Section VI

ABSOLUTE STABILITY AND THE STABILITY REGION OF THE  
SPRING/DAMPER COMPENSATED COUPLED TWO-BODY SYSTEM

As was mentioned in Section II, the nature of the coupled two-body problem is nonlinear even though it was approached by formulating and investigating a linear model. This linearization approach enables one to take full advantage of the simplicity of linear structure for system design and was justified on the basis of Liapunov's first method, that is, linear asymptotic stability implies nonlinear asymptotic stability. However, it should be emphasized that some properties, such as the global property of linear stability generally may not be carried over to the nonlinear model. In fact, nonlinear asymptotic stability is, in general, a local property, that is, not all initial states will result in an asymptotic stable solution. The maximum region in the state space for which every initial state would end up with an asymptotic stable solution is called the (asymptotic) "stability region". Estimation of the stability region is a very important and practical engineering problem even though there are no classical stability theorems which can solve this problem. Liapunov's second method, however, can provide some information, but the "estimation" obtained is strongly dependent on how good a choice is made for the Liapunov function. Generally speaking, the estimated stability region is conservative. One systematic approach (reference 2) is to utilize the quadratic Liapunov function ( $V$ ) based on the linear model. It can be obtained by solving a Liapunov equation and then finding its time derivative ( $\dot{V}_N$ ) with respect to the nonlinear model. An estimation of the stability region is then obtained by finding the largest region in the state space for which  $V$  is positive and  $\dot{V}_N$  is negative (see Figure 6-1). This search-type scheme can be formulated as a mathematical programming problem. The estimate of stability region based on  $V$  is given as

$$\hat{\Omega} = \{ \underline{x} \mid V(\underline{x}) \leq K^* \}$$

where

$$K^* = \min_{\underline{x} \in D} \{ V(\underline{x}) \}$$

and

$$D \equiv \{ \underline{x} \mid \dot{V}_N(\underline{x}) = 0 \} .$$

As the nonlinear terms become more complicated such as with the problem herein, the above procedure becomes increasingly more difficult. Sometimes, however, the nonlinear model could be globally asymptotic-stable, such as the one-dimensional Liénard-type damped harmonic motion with a nonlinear spring (reference 6) which can usually be revealed by physical reasoning. In the following, a heuristic proof on the absolute stability and global stability will be given, which uses physical and system-theoretic reasoning.

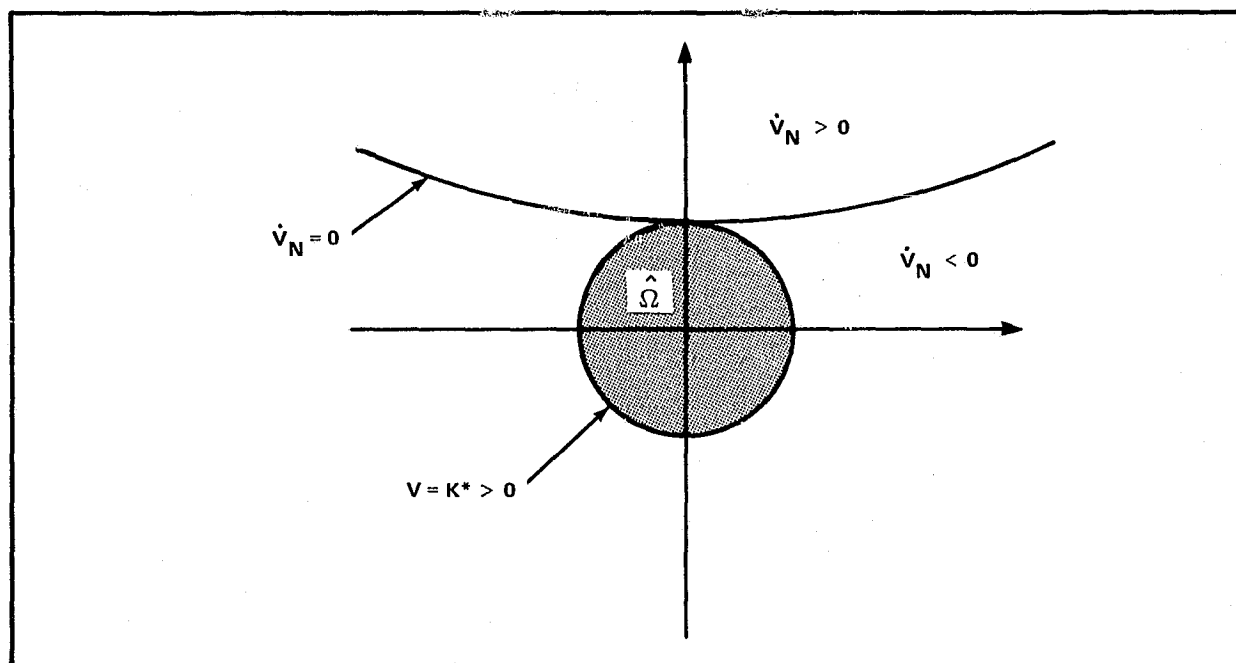


Figure 6-1. STABILITY REGION ESTIMATION BY QUADRATIC LIAPUNOV FUNCTION

First, it is easy to see that all the solutions are bounded. This is because the total energy is finite. Secondly, it should be noted that it is impossible for an equilibrium point with  $\eta \neq 0$  and  $\zeta \neq 0$  to exist. This will become apparent from the following discussion. First, consider the system having the generic form as indicated in Figure 6-2 where the interacting channels may contain some kind of nonlinearity. In mathematical form, one can write

$$\ddot{\eta} = -k\eta - \lambda\dot{\eta} + f_1(\eta, \dot{\eta}, \zeta, \dot{\zeta}, \dot{Y}, \dot{Z})$$

$$\ddot{\zeta} = -k\zeta - \lambda\dot{\zeta} + f_2(\eta, \dot{\eta}, \zeta, \dot{\zeta}, \dot{Y}, \dot{Z})$$

and

$$\ddot{Y} = g_1(\eta, \dot{\eta}, \zeta, \dot{\zeta}, \dot{Y}, \dot{Z})$$

$$\ddot{Z} = g_2(\eta, \dot{\eta}, \zeta, \dot{\zeta}, \dot{Y}, \dot{Z}).$$

Now, when  $\eta = \eta_0$  and  $\zeta = \zeta_0$  where both  $\eta_0$  and  $\zeta_0$  are nonzero constants, then  $\dot{\eta} = 0$  and  $\dot{\zeta} = 0$ . This implies that  $\dot{\theta}_{2y} = \dot{\theta}_{1y} \equiv \dot{\theta}_y$  and  $\dot{\theta}_{2z} = \dot{\theta}_{1z} \equiv \dot{\theta}_z$  and consequently  $\dot{Y} = \dot{\theta}_y$  and  $\dot{Z} = \dot{\theta}_z$ . There are two possibilities for  $\dot{Y}$  and  $\dot{Z}$ : one is that  $\dot{Y}$  and  $\dot{Z}$  are constants and the other is that  $\dot{Y}$  and  $\dot{Z}$  are time varying. An extreme case of the first category will be examined first, namely  $\dot{Y} = 0$  and  $\dot{Z} = 0$  which implies that  $\dot{\theta}_{2y} = \dot{\theta}_{1y} = 0$  and  $\dot{\theta}_{2z} = \dot{\theta}_{1z} = 0$ . Physically, this is a situation for which the relative misalignment between the two bodies is not zero and in addition each body is not rotating about the body y and z axes. Due to the existence of the spring/damper compensation, it is very plausible that this cannot be an equilibrium situation in the  $\eta$ - $\zeta$  plane.

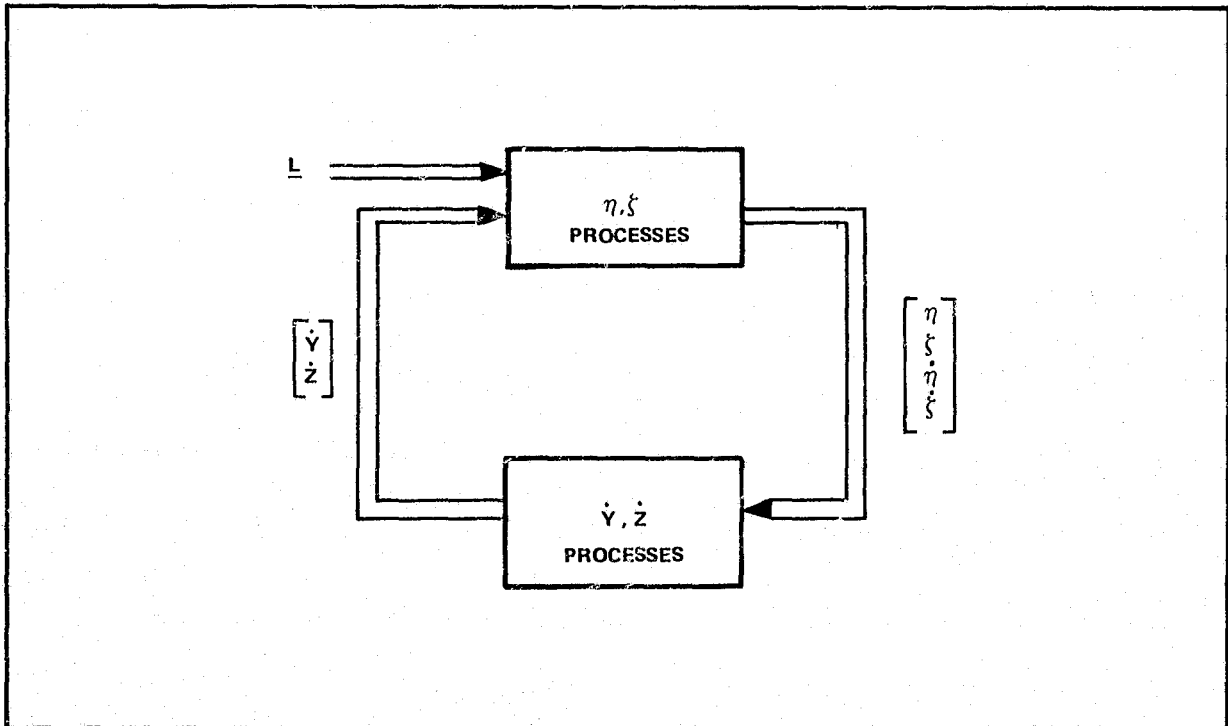


Figure 6-2. GENERAL NONLINEAR STRUCTURE MODEL

Now suppose that  $\dot{Y}_0$  and  $\dot{Z}_0$  are equal to nonzero constants such that

$$\begin{bmatrix} \eta \\ \zeta \end{bmatrix} = \begin{bmatrix} \eta_0 \\ \zeta_0 \end{bmatrix}$$

along with  $\dot{Y}_0$  and  $\dot{Z}_0$  form an equilibrium state. Accordingly, a contradiction to the case with  $\dot{Y} = 0$  and  $\dot{Z} = 0$  is followed by Galilean invariance (reference 9). Next, consider the situation where  $\dot{Y}(t) = \dot{Y}^*(t)$  and  $\dot{Z}(t) = \dot{Z}^*(t)$ , that is,  $\dot{Y}$  and  $\dot{Z}$  are not constants. In order to satisfy  $\dot{\eta} = 0$  and  $\dot{\zeta} = 0$ , then one must have both

$$f_1(\eta_0, 0, \zeta_0, 0, \dot{Y}^*, \dot{Z}^*) = k \eta_0$$

$$f_2(\eta_0, 0, \zeta_0, 0, \dot{Y}^*, \dot{Z}^*) = k \zeta_0$$

and

$$\ddot{Y}^* = g_1(\eta_0, 0, \zeta_0, 0, \dot{Y}^*, \dot{Z}^*)$$

$$\ddot{Z}^* = g_2(\eta_0, 0, \zeta_0, 0, \dot{Y}^*, \dot{Z}^*).$$

Note that under this assumption, the solution to the first two of these algebraic equations should not be unique. In particular, some constant solutions for  $\dot{Y}$  and  $\dot{Z}$  do exist. For example, if  $\dot{Y} = \dot{Y}^\dagger$  and  $\dot{Z} = \dot{Z}^\dagger$  are taken as constant solutions, then

$$f_1(\eta_0, 0, \zeta_0, 0, \dot{Y}^\dagger, \dot{Z}^\dagger) = f_1(\eta_0, 0, \zeta_0, 0, \dot{Y}^*, \dot{Z}^*) = k \eta_0$$

and

$$f_2(\eta_0, 0, \zeta_0, 0, \dot{Y}^\dagger, \dot{Z}^\dagger) = f_2(\eta_0, 0, \zeta_0, 0, \dot{Y}^*, \dot{Z}^*) = k \zeta_0.$$

In other words, one can imagine that the  $\eta, \zeta$  subsystem has constant inputs as indicated in Figure 6-3. However, this turns out to be the same situation as the first category which has already been shown to be impossible. So, the nonexistence of equilibrium points with nonzero misalignments has thus been shown.

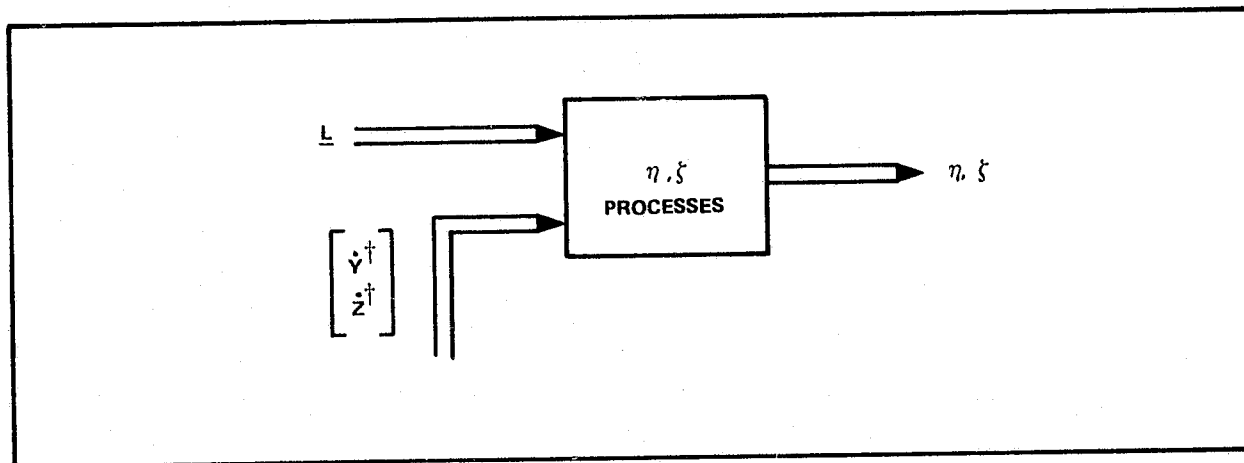


Figure 6-3. A DECOMPOSED VIEW

Finally, the possibility of a limit cycle type instability is considered. Suppose that the stability is not global and that an initial state outside the stability region might result in a trajectory oscillating along a limit cycle. Owing to the energy dissipation through damping, the oscillation period must become longer and longer with both  $|\dot{\eta}|$  and  $|\dot{\zeta}|$  going to zero as time goes to infinity. This situation then approaches the situation discussed before, that is, the nonzero misalignment equilibrium point which has been shown to be impossible.

In the above discussion, it has been shown that any initial state would result in zero misalignment in the  $\eta, \zeta$  space, that is, the stability is global. Meanwhile, no particular values of  $k$  and  $\lambda$  were assumed so absolute stability is also proven as a general result. To look at absolute stability for the case where body 1 has x-directional attitude control, very small spring/damper constants were selected. These numerical results are presented in Table 6-1 from which it can be seen that, as long as  $\bar{k} > 0$  and  $\bar{\lambda} > 0$ , then the system is (at least in principle) asymptotically stable.

Table 6-1. POLES FOR SMALL SPRING/DAMPER CONSTANTS

SPRING/DAMPER	POLES
$\bar{k} = 0$ $\bar{\lambda} = 2. \times 10^{-5}$	$0, 0$ $-0.17803 \times 10^{-4} \pm 0.27674j$ $-0.21965 \times 10^{-5} \pm 0.14030 \times 10^{-9}j$
$\bar{k} = 1. \times 10^{-12}$ $\bar{\lambda} = 2. \times 10^{-5}$	$-0.46185, - 0.56772$ $-0.17803 \times 10^{-4} \pm 0.27674j$ $-0.21108 \times 10^{-5} \pm 0.21993j$
$\bar{k} = 1. \times 10^{-10}$ $\bar{\lambda} = 2. \times 10^{-5}$	$-0.10981 \times 10^{-5} \pm 0.31266 \times 10^{-5}j$ $-0.17803 \times 10^{-4} \pm 0.27674j$ $-0.10984 \times 10^{-5} \pm 0.31268 \times 10^{-5}j$
$\bar{k} = 1. \times 10^{-10}$ $\bar{\lambda} = 2. \times 10^{-7}$	$-0.10976 \times 10^{-7} \pm 0.33138 \times 10^{-5}j$ $-0.17803 \times 10^{-6} \pm 0.27674j$ $-0.10984 \times 10^{-7} \pm 0.33141 \times 10^{-5}j$
$\bar{k} = 1. \times 10^{-10}$ $\bar{\lambda} = 0$	$0 \pm 0.33138 \times 10^{-5}j$ $0 \pm 0.27674j$ $0 \pm 0.33141 \times 10^{-5}j$

## Section VII

## SIMULATION RESPONSE STUDY

## 7.1 GENERAL

A digital computer simulation called 2BODY (reference 10) was developed for studying the post-docking behavior of the Space Tug during recovery of a spinning satellite. The simulation accounts for the translational as well as the rotational motion of both the Tug and a target vehicle. The two vehicles are modeled as rigid bodies physically attached at a single point about which relative rotation between these two bodies is permitted. In addition, the target vehicle is allowed the freedom to spin about an axis in the proximity of the docking port axis. Such a configuration is analogous to the soft-dock regime wherein capture or initial latch has been achieved but final latch or hard-dock has not. Options relative to vehicle dynamics include ideal 3-axis attitude control of the chase vehicle, a spring/damper type alignment torque applied at the joint between the vehicles, and a despin torquer for despinning a spinning payload. These nonlinear models are described in more detail in Appendix D. This simulation, providing both digital and graphical output was used to study the dynamical behavior of various post-docked configurations as well as to verify the results of the analytical stability presented previously in Part I, Sections II through VI.

## 7.2 SIMULATION RESULTS

Simulation studies were performed to answer several questions concerning post-dock behavior during the recovery of a spinning satellite. The primary concern was to determine whether the post-docked configuration is stable and well-behaved for various:

- target inertia characteristics
- alignment spring/damper characteristics
- despin torquer limits.

Figures 7-1 and 7-2 show the overall results of these studies for an uncontrolled Tug and for one with perfect attitude control respectively. Three target inertias are considered: a disk, an end-dock cylinder and a

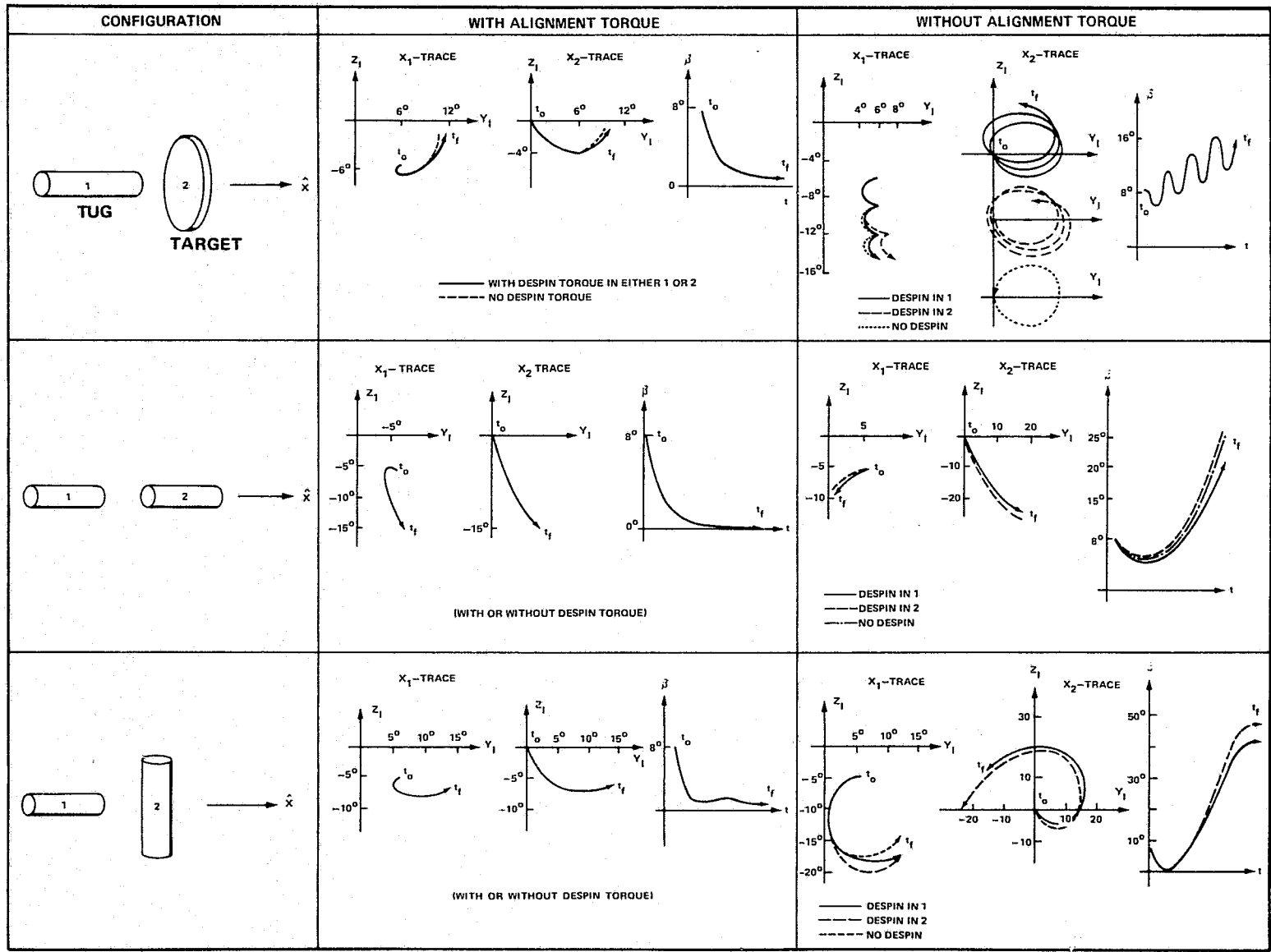


Figure 7-1. TWO-BODY BEHAVIOR FOR UNCONTROLLED TUG



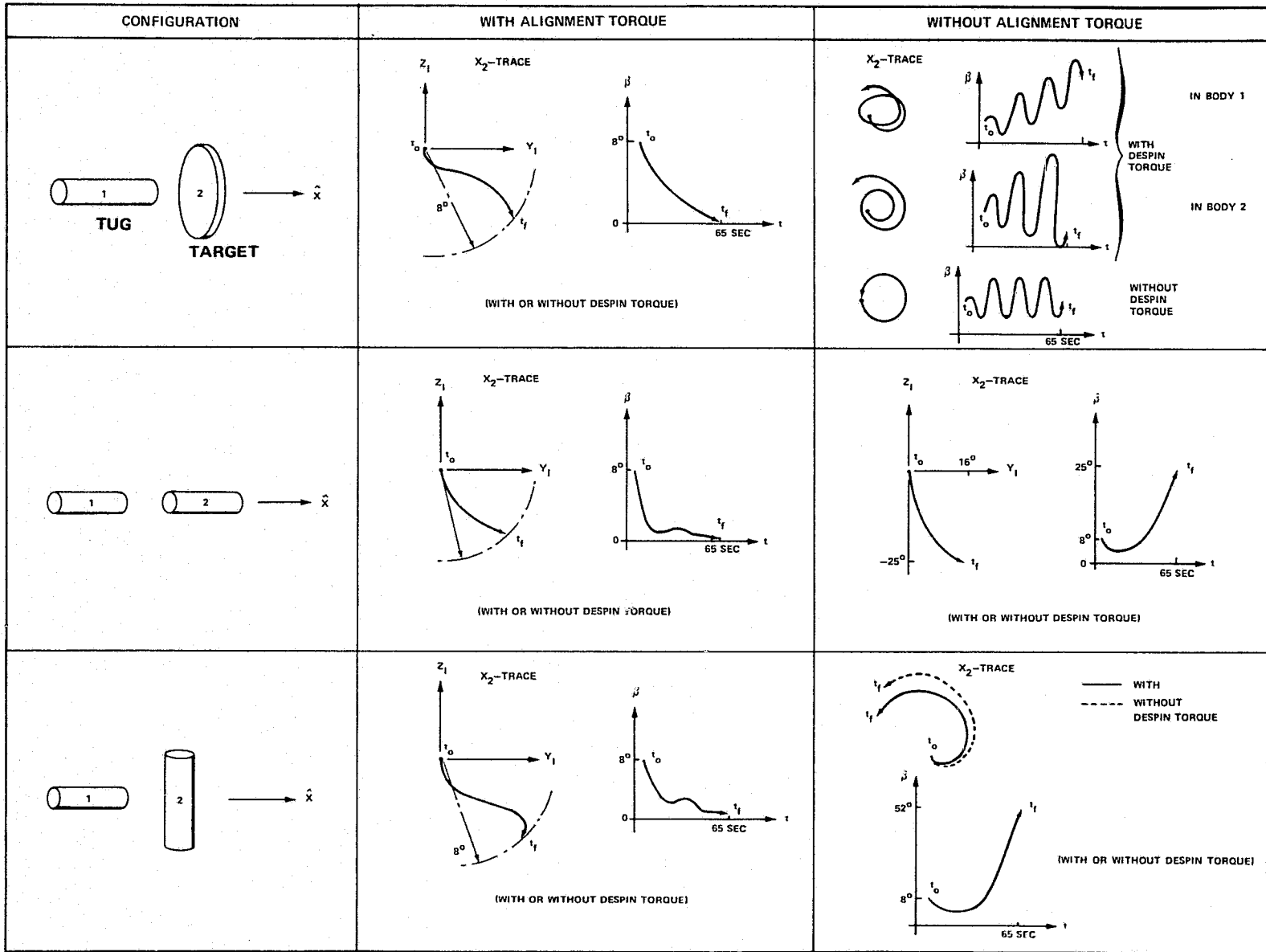


Figure 7-2. TWO-BODY BEHAVIOR FOR TUG 3-AXIS ATTITUDE CONTROL

side-dock cylinder. In each case the target is assumed to be initially at a constant angular rate about the docking port centerline with some misalignment and wobble. The response curves show qualitatively the parametric angular motion of the target centerline in inertial space and the time response of the angle  $\beta$  between the Tug and target vehicle centerlines, with and without alignment springs and dampers.

The results in Figure 7-1 show that the uncontrolled post-dock configuration is stable for all three types of targets, provided alignment springs and dampers are present. The motion of both centerlines is well behaved and the alignment angle tends toward zero in all cases. The righthand column in Figure 7-1 illustrates the fact that the post-dock configuration tends to be unstable without alignment springs and dampers. The angle between the two centerlines diverges indicating the tendency of the two vehicles to pitch and yaw into each other. Figure 7-2 shows that alignment springs and dampers are still necessary even when the Tug has ideal attitude control.

Alignment damping and natural frequency were parameterized as was despin torque to determine appropriate settings. Figure 7-3 shows the behavior of the misalignment angle  $\beta$  for several damping ratios with all other conditions held constant. The conclusion is that critical damping ( $\zeta = 1.0$ ) is best in driving misalignment quickly to zero with a minimum of oscillation. Natural frequency  $f_n$  should be as high as possible for fast settling time, as shown in Figure 7-4, but will be limited by the weight of the springs in relation to vehicle weights.

The rate of despin is linearly proportional to despin torque. A despin torque of 100 ft-lb can despin the target from 0.1 rad/sec to zero in approximately 43 seconds and one third of a revolution. Lower torques require longer times to despin as shown in Figure 7-5, but in no case is there a stability problem, provided alignment springs and dampers are used. Despin torque was applied about the centerline of the Tug as well as the target vehicle with little difference noted in the response. The conclusion is that the exact direction and magnitude of despin torque are not critical.

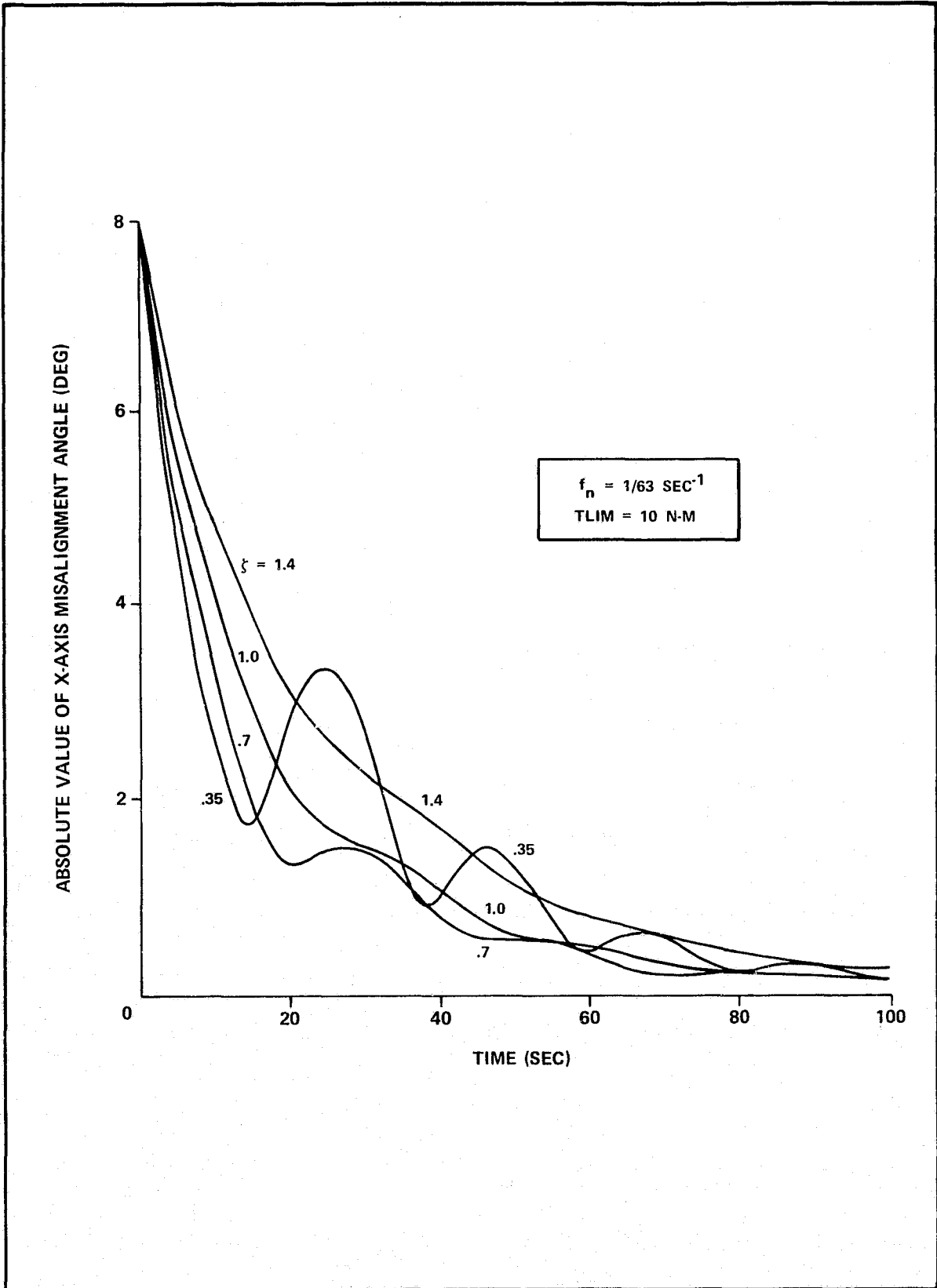


Figure 7-3. DAMPING EFFECT

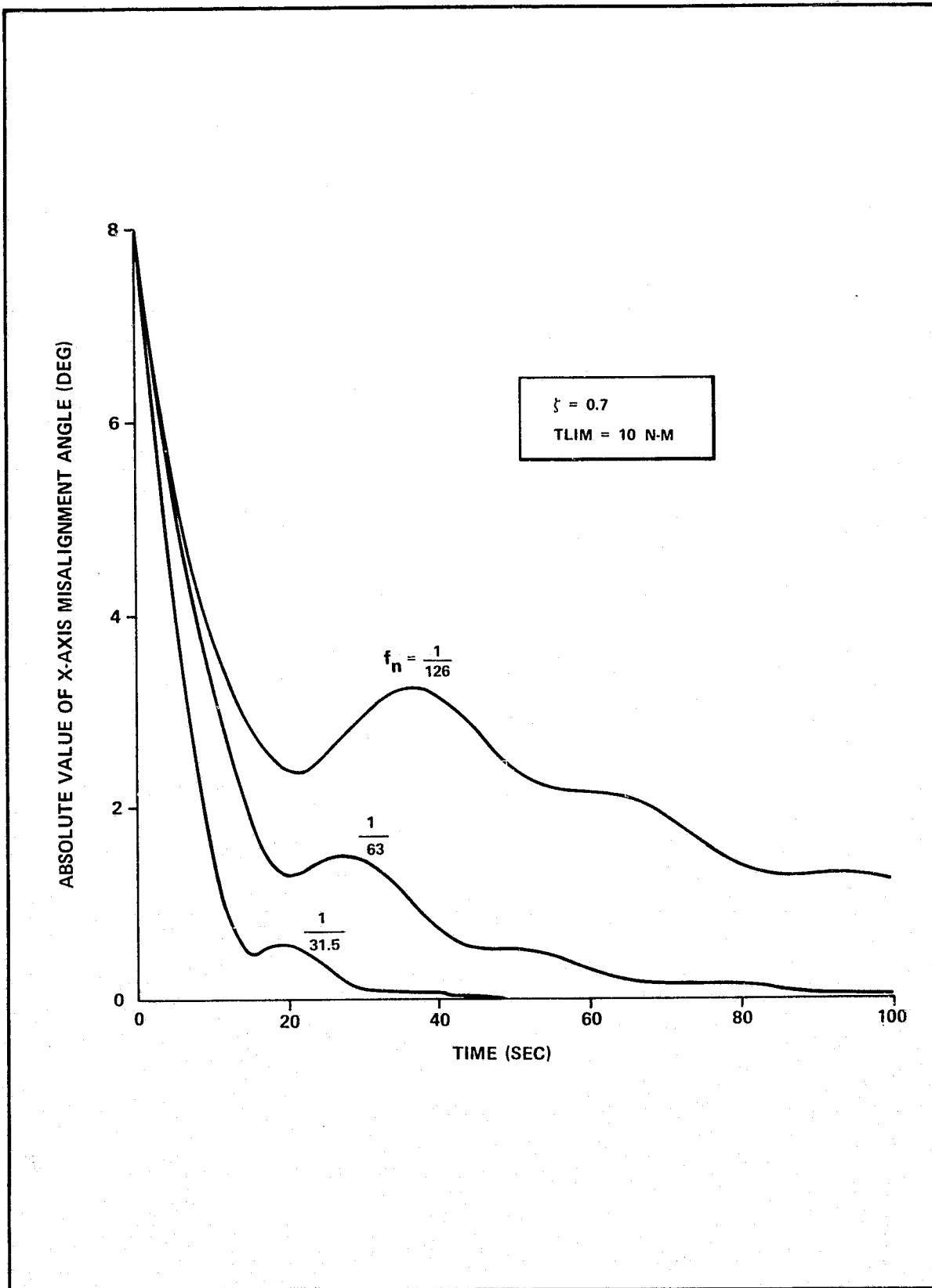


Figure 7-4. ALIGNMENT NATURAL FREQUENCY EFFECT

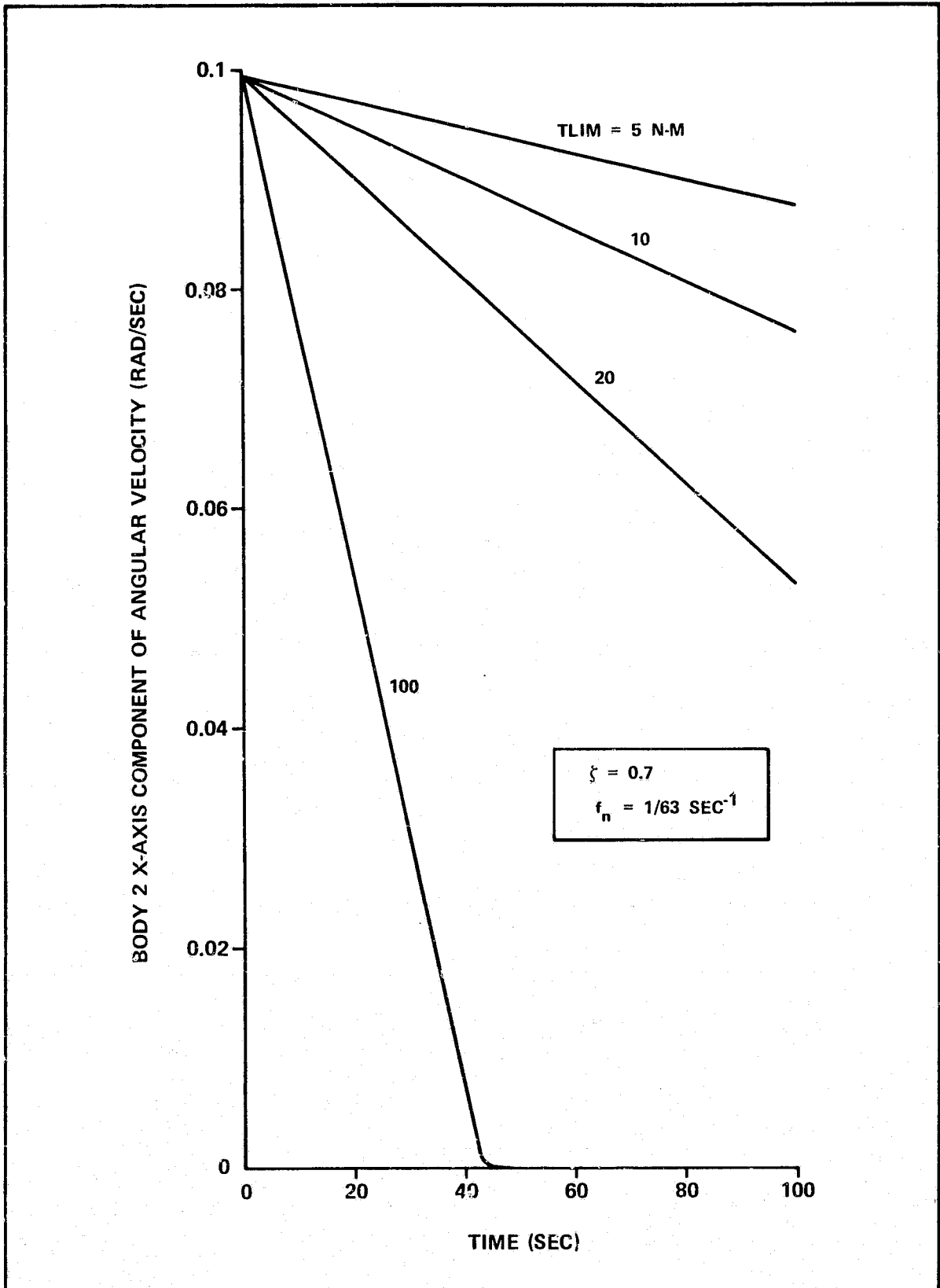


Figure 7-5. DESPIN TORQUE EFFECT

## Section VIII

## SUMMARY, CONCLUSIONS, AND DISCUSSION

In summary, the objective of the study documented heretofore was to investigate the stability and response of both the Tug and a spinning satellite while attached together in a soft-docked configuration. The behavior of this coupled two-body system was to be assessed relative to mass/inertia characteristics, a spring/damper alignment torque, a despin torque, and ideal 3-axis Tug attitude control. The approach taken in this analysis has been two-fold: an analytical stability study based primarily on a linear model and a simulation response study based on a nonlinear model.

Table 8-1 shows three types of Tug/payload configurations and an indication of the analytic and numeric studies performed for each. It should be noted that although the numerical stability results were based primarily on a nominal model, analytical inference was used to make them as parameter independent as possible. Therefore, the analytical stability results based on the linear model are, in general, valid for both the disk and end-dock payloads. Table 8-2 summarizes the analytical stability results which are applicable to either of the first two Tug/payload configurations indicated in Table 8-1. These stability results (Table 8-2) are what has been deduced for the nonlinear system as determined from the linear model based on Liapunov's first method (see subsection 2.1). It should be noted that in Table 8-2, asymptotic stability is taken to mean Liapunov stable as time approaches infinity and such stability is not necessarily inferred near zero time. The simulation study verified as expected that:

- An alignment torque damping factor in the proximity of critical damping is best for reducing misalignment between the docking port axes to zero with a minimum of oscillation.
- An alignment torque natural frequency should be as high as possible for fast settling time, but will obviously be limited by structural weight considerations.
- The despin time is linearly proportional to the despin torque (for a reasonable range of values) with a smaller torque requiring a longer despin time.

Table 8-1. CONFIGURATIONS STUDIED

TUG/PAYLOAD CONFIGURATION	ANALYTIC STUDY	NUMERIC STUDY
<p>TUG</p> <p>DISK PAYLOAD</p>	<p>✓</p>	<p>✓</p>
<p>TUG</p> <p>END-DOCK PAYLOAD</p>	<p>✓</p>	<p>✓</p>
<p>TUG</p> <p>SIDE-DOCK PAYLOAD</p>	<p>—</p>	<p>✓</p>

Table 8-2. ANALYTICAL STABILITY STUDY RESULTS

ALIGNMENT TORQUE	DESPIN TORQUE	TUG ATTITUDE CONTROL		
		NONE	X-AXIS ONLY	3-AXIS
NO	NO	NO CONCLUSION (FOR NONLINEAR MODEL)	UNSTABLE	NO CONCLUSION (FOR NONLINEAR MODEL)
YES	NO	ABSOLUTELY STABLE	ABSOLUTELY STABLE	ABSOLUTELY STABLE
NO	YES	UNSTABLE	UNSTABLE	UNSTABLE
YES	YES	ASYMPTOTICALLY STABLE	ASYMPTOTICALLY STABLE	ASYMPTOTICALLY STABLE



It may be concluded that, for the cases studied, the two-body coupled system is stable as long as some dissipative/energy storage (spring/damper) alignment torque exist. In addition, no system instability is encountered for reasonable values of despin torque.

In the foregoing studies, it was found that the results derived from the nonlinear simulation agreed well with those predicted by the linear analytical stability analysis. However, it should be understood that the linear analytical model and the nonlinear simulation model have different functions. And because of their inherent advantages and disadvantages, a judiciously combined utilization of the two provides the greatest amount of information and is therefore essential to an efficient and successful analysis and design.

In general, the analytic model has the advantages of providing not only stability information (except for a few open-loop cases), but also a design guideline, an understanding of system structure, and therefore possibly parametric effects. The disadvantages include a loss of generality (for instance, there is no simple exact linearized model for the side-dock payload configuration depicted in Table 8-1) and a loss of time fidelity (nonlinearities are absent). On the other hand, the simulation model has the advantages of providing both more genuine results (nonlinear effects are taken into account) and information for more complicated cases (like the above mentioned case involving a side-dock target). Also, it is suitable for parametric studies.

## Section IX

## REFERENCES

1. Ogata, K., State Space Analysis of Control Systems, Prentice-Hall, Inc., 1967.
2. Schultz, D. G. and J. L. Melsa, State Functions and Linear Control Systems, McGraw-Hill, Inc., 1967.
3. Zadeh, L. A. and C. A. Desoer, Linear System Theory - The State Space Approach, McGraw-Hill, Inc., 1963.
4. Space Tug Recovery of Spinning Satellite, Part I - Technical Proposal, Northrop Services, Inc., NSI-73-8, PS-205-1210, 1973.
5. Gibson, J. E., Nonlinear Automatic Control, McGraw-Hill, Inc., 1963.
6. Brauer, F. and J. A. Nohel, Qualitative Theory of Ordinary Differential Equations, W. A. Benjamin, Inc., 1969.
7. Brockett, R. W., Finite Dimensional Linear Systems, John Wiley, Inc., 1970.
8. Mesarović, M. D., The Control of Multivariable Systems, Technology Press of MIT, 1960.
9. Feynman, R. P., Lecture on Physics, Vol. 1, Addison Wesley, Inc., 1963.
10. Roberts, James R. and Todd, Robert S., "Digital Simulation for Post-Docking Response," Northrop Services, Inc., Huntsville, Alabama, Technical Report, TR-250-1378, December 1974.

Appendix A

GENERAL EQUATIONS OF MOTION FOR TWO COUPLED RIGID BODIES

The general rotational equations of motion for two rigid bodies connected at a single point as shown in Figure D-1 is given by a (6 x 1) matrix equation as

$$J \dot{\omega} = \ell$$

where

$$J = \begin{bmatrix} I_1^* & & K \\ & & \\ K^T & & I_2^* \end{bmatrix}, \quad \dot{\omega} = \begin{bmatrix} \dot{\omega}_1 \\ \dot{\omega}_2 \end{bmatrix}, \quad \ell = \begin{bmatrix} \ell_1 \\ \ell_2 \end{bmatrix}$$

and

$$I_i^* = I_i - \mu \tilde{d}_i \tilde{d}_i, \quad i=1,2$$

$$K = \mu \tilde{d}_1 T' \tilde{d}_2$$

$$\ell_1 = \ell_1^* + L_1 + \tilde{d}_1 F_1^* - \tilde{\omega}_1 I_1 \omega_1$$

$$\ell_2 = \ell_2^* - L_2 - \tilde{d}_2 F_2^* - \tilde{\omega}_2 I_2 \omega_2$$

$$F_1^* = \frac{m_1}{m} T' f_2 - \frac{m_2}{m} f_1 + \mu T' \tilde{\omega}_2 \tilde{\omega}_2 \tilde{d}_2 - \mu \tilde{\omega}_1 \tilde{\omega}_1 \tilde{d}_1$$

$$m = m_1 + m_2$$

$$\mu = m_1 m_2 / m$$

$I_i$  - (3x3) inertia matrix for body i, i = 1, 2

$\tilde{d}_i$  - (3x1) column matrix of the joint vector components for body i, i = 1, 2 (the joint vector is from the center of mass of body i to the hinge point between the two bodies)

$T'$  - (3x3) coordinate transformation matrix resolving a vector defined in the body 2 reference frame into the body 1 reference frame, that is,  $F_1^* = T' F_2^*$

$\omega_i$  - (3x1) column matrix of the angular velocity components of body i, i = 1, 2

$\ell_i^*$  - (3x1) column matrix of the total external torque components acting on body i, i = 1, 2

$f_i$  - (3x1) column matrix of the total external force components acting on body  $i$ ,  $i = 1, 2$

$L_i$  - (3x1) column matrix of the joint torque components acting on body  $i$ ,  $i = 1, 2$

It should be noted that the tilde ( $\sim$ ) placed over the symbol for a column vector indicates the 3-dimensional vector cross product operator, which for any vector

$$V = \begin{bmatrix} V_x \\ V_y \\ V_z \end{bmatrix}$$

is defined as

$$\tilde{V} = \underline{V} \times \equiv \begin{bmatrix} 0 & -V_z & V_y \\ V_z & 0 & -V_x \\ -V_y & V_x & 0 \end{bmatrix}.$$

## Appendix B

SIMPLIFIED LINEARIZED EQUATIONS OF MOTION  
FOR TWO COUPLED RIGID BODIES

In Appendix A, a summary of the completely general nonlinear equations of motion for two coupled rigid bodies was given. In the appendix herein, these equations of motion will be simplified according to the following assumptions:

- No external forces or torques are assumed to act on either of the two bodies. Therefore,

$$f_1 = f_2 = \ell_1^* = \ell_2^* = 0$$

and the expressions for  $\ell_1$ ,  $\ell_2$ , and  $F_1^*$  in Appendix A reduce to

$$\ell_1 = L_1 + \tilde{d}_1 F_1^* - \tilde{\omega}_1 I_1 \omega_1$$

$$\ell_2 = -L_2 - \tilde{d}_2 F_2^* - \tilde{\omega}_2 I_2 \omega_2$$

$$F_1^* = \mu (T' \tilde{\omega}_2 \tilde{\omega}_2 d_2 - \tilde{\omega}_1 \tilde{\omega}_1 d_1).$$

- The equations of motion are linearized with respect to rotations about the y and z axes. That is, the angles  $\theta_{iy}$  and  $\theta_{iz}$  ( $i=1,2$ ) are assumed small such that the following small angle approximations can be made:

$$\sin \theta_{iy} \cong \theta_{iy}, \quad \sin \theta_{iz} \cong \theta_{iz},$$

$$\cos \theta_{iy} \cong 1, \quad \cos \theta_{iz} \cong 1.$$

In addition, the products of small angles and their rates are neglected, i.e.,  $\theta_{iy}^2$ ,  $\theta_{iz}^2$ ,  $\theta_{iy} \theta_{iz}$ ,  $\dot{\theta}_{iy}^2$ ,  $\dot{\theta}_{iz}^2$ ,  $\dot{\theta}_{iy} \dot{\theta}_{iz}$ ,  $\theta_{iy} \dot{\theta}_{iz}$ , and  $\dot{\theta}_{iy} \theta_{iz}$  are all assumed equal to zero. The coordinate transformation matrix between the inertial frame and body i ( $i = 1, 2$ ) is developed from a 3-2-1 Euler angle sequence going from the inertial to the body i reference frame, that is,

$$\{x\}_I = [-\theta_{iz}] [-\theta_{iy}] [-\theta_{ix}] \{x\}_i = T_i \{x\}_i$$

where the nonlinear and linearized single axis rotation matrices are defined as

$$[-\theta_{ix}] = \begin{bmatrix} 1 & 0 & 0 \\ 0 & \cos \theta_{ix} & -\sin \theta_{ix} \\ 0 & \sin \theta_{ix} & \cos \theta_{ix} \end{bmatrix}, \quad [-\theta_{iy}] = \begin{bmatrix} 1 & 0 & \theta_{iy} \\ 0 & 1 & 0 \\ -\theta_{iy} & 0 & 1 \end{bmatrix},$$

and

$$[-\theta_{iz}] = \begin{bmatrix} 1 & -\theta_{iz} & 0 \\ \theta_{iz} & 1 & 0 \\ 0 & 0 & 1 \end{bmatrix}.$$

Therefore

$$T_i = \begin{bmatrix} 1 & \theta_{iy} \sin\theta_{ix} - \theta_{iz} \cos\theta_{ix} & \theta_{iy} \cos\theta_{ix} + \theta_{iz} \sin\theta_{ix} \\ \theta_{iz} & \cos\theta_{ix} & -\sin\theta_{ix} \\ -\theta_{iy} & \sin\theta_{ix} & \cos\theta_{ix} \end{bmatrix}.$$

From the kinematical relationship,

$$\dot{T}_i = T_i \tilde{\omega}_i,$$

the angular velocity of body  $i$  ( $i = 1, 2$ ) is obtained as follows

$$\omega_i = \begin{bmatrix} \dot{\theta}_{ix} \\ \dot{\theta}_{iy} \cos\theta_{ix} + \dot{\theta}_{iz} \sin\theta_{ix} \\ \dot{\theta}_{iz} \cos\theta_{ix} - \dot{\theta}_{iy} \sin\theta_{ix} \end{bmatrix} = [-\theta_{ix}]^T \begin{bmatrix} \dot{\theta}_{ix} \\ \dot{\theta}_{iy} \\ \dot{\theta}_{iz} \end{bmatrix} = [\theta_{ix}] \begin{bmatrix} \dot{\theta}_{ix} \\ \dot{\theta}_{iy} \\ \dot{\theta}_{iz} \end{bmatrix}$$

- The body fixed reference frames are assumed to be principal axes of inertia. Therefore, the body inertia matrix of body  $i$  ( $i = 1, 2$ ) can be written as

$$I_i = \begin{bmatrix} A_i & 0 & 0 \\ 0 & B_i & 0 \\ 0 & 0 & C_i \end{bmatrix}.$$

- Each body is assumed to be symmetrical about the body  $x$ -axis with respect to inertia, that is,  $B_i = C_i$  for  $i = 1, 2$ . Therefore, the inertia matrix of each body is further reduced to

$$I_i = \begin{bmatrix} A_i & 0 & 0 \\ 0 & C_i & 0 \\ 0 & 0 & C_i \end{bmatrix}.$$

- The center of mass of each body is assumed to lie on the x-axis.
- The joint or hinge connecting the two bodies is also assumed to lie on the x-axis. Therefore, the joint vectors  $\underline{d}_1$  and  $\underline{d}_2$  in their respective body reference frames can be expressed as

$$d_i = \begin{bmatrix} d_{ix} \\ 0 \\ 0 \end{bmatrix}, i = 1, 2.$$

Based on the above simplifying assumptions, the matrix equation (equation (A-1)) given in Appendix A, describing the rotational motion of two coupled rigid bodies connected at a single point, expanded in scalar form can be written as

$$\begin{aligned} A_1 \ddot{\theta}_{1x} &= L_{1x} \\ C_1^*(\ddot{\theta}_{1y} + \dot{\theta}_{1z} \dot{\theta}_{1x}) - K(\ddot{\theta}_{2y} + \dot{\theta}_{2z} \dot{\theta}_{2x}) &= L_{1y} \cos \theta_{1x} - L_{1z} \sin \theta_{1x} \\ &\quad - (A_1 - C_1) \dot{\theta}_{1z} \dot{\theta}_{1x} - \mu d_{1x} (d_{2x} \dot{\theta}_{2z} \dot{\theta}_{2x} - d_{1x} \dot{\theta}_{1z} \dot{\theta}_{1x}) \\ C_1^*(\ddot{\theta}_{1z} - \dot{\theta}_{1y} \dot{\theta}_{1x}) - K(\ddot{\theta}_{2z} - \dot{\theta}_{2y} \dot{\theta}_{2x}) &= L_{1y} \sin \theta_{1x} + L_{1z} \cos \theta_{1x} \\ &\quad + (A_1 - C_1) \dot{\theta}_{1y} \dot{\theta}_{1x} + \mu d_{1x} (d_{2x} \dot{\theta}_{2y} \dot{\theta}_{2x} - d_{1x} \dot{\theta}_{1y} \dot{\theta}_{1x}) \\ A_2 \ddot{\theta}_{2x} &= -L_{2x} \tag{B-1} \\ C_2^*(\ddot{\theta}_{2y} + \dot{\theta}_{2z} \dot{\theta}_{2x}) - K(\ddot{\theta}_{1y} + \dot{\theta}_{1z} \dot{\theta}_{1x}) &= -L_{2y} \cos \theta_{2x} + L_{2z} \sin \theta_{2x} \\ &\quad - (A_2 - C_2) \dot{\theta}_{2z} \dot{\theta}_{2x} + \mu d_{2x} (d_{2x} \dot{\theta}_{2z} \dot{\theta}_{2x} - d_{1x} \dot{\theta}_{1z} \dot{\theta}_{1x}) \\ C_2^*(\ddot{\theta}_{2z} - \dot{\theta}_{2y} \dot{\theta}_{2x}) - K(\ddot{\theta}_{1z} - \dot{\theta}_{1y} \dot{\theta}_{1x}) &= -L_{2y} \sin \theta_{2x} - L_{2z} \cos \theta_{2x} \\ &\quad + (A_2 - C_2) \dot{\theta}_{2y} \dot{\theta}_{2x} - \mu d_{2x} (d_{2x} \dot{\theta}_{2y} \dot{\theta}_{2x} - d_{1x} \dot{\theta}_{1y} \dot{\theta}_{1x}) \end{aligned}$$

where

$$C_i^* = C_i + \mu d_{ix}^2, i=1,2.$$

From

$$L_2 = T_2^{-1} T_1 L_1$$

then

$$L_{2x} = L_{1x} + \left[ (\theta_{2z} - \theta_{1z}) \cos \theta_{1x} - (\theta_{2y} - \theta_{1y}) \sin \theta_{1x} \quad L_{1y} \right] \\ - \left[ (\theta_{2y} - \theta_{1y}) \cos \theta_{1x} + (\theta_{2z} - \theta_{1z}) \sin \theta_{1x} \quad L_{1z} \right] \quad (B-2)$$

Since  $\theta_{1y}$  and  $\theta_{1z}$  are assumed to be small angles, it is reasonable to assume that the torques  $L_{1y}$  and  $L_{1z}$  will also be small in comparison to  $L_{1x}$ . Consequently a first order approximation of equation (B-2) is

$$L_{2x} \cong L_{1x}$$

and the first and fourth equation of (B-1) becomes

$$A_1 \ddot{\theta}_{1x} = -A_2 \ddot{\theta}_{2x} = L_{1x}.$$

If in addition, it is assumed that  $L_{1x} = L_{1x}(\theta_{1x}, \theta_{2x}, t)$ , then these two equations decouple from the other four equations of (B-1) and can be solved separately. Therefore, the values of  $\theta_{1x}$  ( $i = 1, 2$ ) and their derivatives can be regarded as known functions of time in the remaining four equations. Since the other four equations are linear in the other variables, they can be written in matrix form as

$$\hat{J} \ddot{\theta} + \hat{K} \dot{\theta} = \hat{L} \quad (B-3)$$

where

$$\hat{J} = \begin{bmatrix} C_1^* & 0 & -K & 0 \\ 0 & C_1^* & 0 & -K \\ -K & 0 & C_2^* & 0 \\ 0 & -K & 0 & C_2^* \end{bmatrix},$$



$$\hat{K} = \begin{bmatrix} 0 & A_1 \dot{\theta}_{1x} & 0 & 0 \\ -A_1 \dot{\theta}_{1x} & 0 & 0 & 0 \\ 0 & 0 & 0 & A_2 \dot{\theta}_{2x} \\ 0 & 0 & -A_2 \dot{\theta}_{2x} & 0 \end{bmatrix}$$

$$\ddot{\theta} = \begin{bmatrix} \ddot{\theta}_{1y} \\ \ddot{\theta}_{1z} \\ \ddot{\theta}_{2y} \\ \ddot{\theta}_{2z} \end{bmatrix}, \quad \dot{\theta} = \begin{bmatrix} \dot{\theta}_{1y} \\ \dot{\theta}_{1z} \\ \dot{\theta}_{2y} \\ \dot{\theta}_{2z} \end{bmatrix}, \quad \text{and } \hat{L} = \begin{bmatrix} \hat{L}_{1y} \\ \hat{L}_{1z} \\ -\hat{L}_{2y} \\ -\hat{L}_{2z} \end{bmatrix}$$

where

$$\left. \begin{aligned} \hat{L}_{iy} &= L_{iy} \cos \theta_{ix} - L_{iz} \sin \theta_{ix} \\ \hat{L}_{iz} &= L_{iy} \sin \theta_{ix} + L_{iz} \cos \theta_{ix} \end{aligned} \right\}, \quad i = 1, 2.$$

## Appendix C

## SIMPLIFIED LINEARIZED EQUATIONS OF MOTION FOR TWO COUPLED RIGID BODIES IN TERMS OF NEW VARIABLES

The two-body equations of motion as developed in Appendix B are in terms of the Euler angles  $\theta_{1y}$ ,  $\theta_{2y}$ ,  $\theta_{1z}$ , and  $\theta_{2z}$ , and their rates and accelerations. Since the interest herein is concerned with the misalignment of the vehicle x-axes, it would be desirable to reexpress these two-body equations of motion in terms of  $\eta = \theta_{2y} - \theta_{1y}$  and  $\zeta = \theta_{2z} - \theta_{1z}$ , which provides a measure of misalignment directly. In addition, these two parameters are ones which can actually be sensed.

In order to facilitate the above change of variables, it becomes necessary to define an additional set of variables, namely

$$\begin{aligned} X &= \alpha \theta_{1x} + (1-\alpha)\theta_{2x} \\ Y &= \alpha \theta_{1y} + (1-\alpha)\theta_{2y} \\ Z &= \alpha \theta_{1z} + (1-\alpha)\theta_{2z} \end{aligned}$$

These variables are analogous to center of mass coordinates where  $\alpha$  is a parameter yet to be determined. Combining the above definitions for  $\eta$ ,  $\zeta$ ,  $Y$ , and  $Z$  results in

$$\begin{bmatrix} Y \\ Z \\ \eta \\ \zeta \end{bmatrix} = \begin{bmatrix} \alpha & 0 & 1-\alpha & 0 \\ 0 & \alpha & 0 & 1-\alpha \\ -1 & 0 & 1 & 0 \\ 0 & -1 & 0 & 1 \end{bmatrix} \begin{bmatrix} \theta_{1y} \\ \theta_{1z} \\ \theta_{2y} \\ \theta_{2z} \end{bmatrix} = B\theta$$

and inverting gives

$$\theta = B^{-1} \begin{bmatrix} Y \\ Z \\ \eta \\ \zeta \end{bmatrix}$$

The two-body equations of motion given by equation (B-3) can now be written as

$$\hat{J} B^{-1} \begin{bmatrix} \ddot{Y} \\ \ddot{Z} \\ \ddot{\eta} \\ \ddot{\zeta} \end{bmatrix} + \hat{K} B^{-1} \begin{bmatrix} \dot{Y} \\ \dot{Z} \\ \dot{\eta} \\ \dot{\zeta} \end{bmatrix} = \hat{L} \quad (C-1)$$

or

$$\begin{bmatrix} \ddot{Y} \\ \ddot{Z} \\ \ddot{\eta} \\ \ddot{\zeta} \end{bmatrix} + (\hat{J} B^{-1})^{-1} \hat{K} B^{-1} \begin{bmatrix} \dot{Y} \\ \dot{Z} \\ \dot{\eta} \\ \dot{\zeta} \end{bmatrix} = (\hat{J} B^{-1})^{-1} \hat{L} = \hat{F} \quad (C-2)$$

Expanding  $\hat{F}$  results in

$$\hat{F} = \frac{1}{\Delta} \begin{bmatrix} [\alpha C_2^* + (1 - \alpha)K] \hat{L}_{1y} - [(1 - \alpha)C_1^* + \alpha K] \hat{L}_{2y} \\ [\alpha C_2^* + (1 - \alpha)K] \hat{L}_{1z} - [(1 - \alpha)C_1^* + \alpha K] \hat{L}_{2z} \\ (K - C_2^*) \hat{L}_{1y} + (K - C_1^*) \hat{L}_{2y} \\ (K - C_2^*) \hat{L}_{1z} + (K - C_1^*) \hat{L}_{2z} \end{bmatrix}.$$

In order to simplify  $\hat{F}$ ,  $\alpha$  is chosen such that the first two elements of  $\hat{F}$  vanish whenever  $\hat{L}_{1y} = \hat{L}_{2y}$  and  $\hat{L}_{1z} = \hat{L}_{2z}$ .

Therefore,

$$[\alpha C_2^* + (1 - \alpha) K] = [(1 - \alpha) C_1^* + \alpha K]$$

from which

$$\alpha = \frac{a_1}{a_1 + a_2}$$

where  $a_1 = C_1^* - K$  and  $a_2 = C_2^* - K$ .

Equation (C-2) can now be written as

$$\begin{bmatrix} \ddot{Y} \\ \ddot{Z} \\ \ddot{\eta} \\ \ddot{\zeta} \end{bmatrix} + \begin{bmatrix} 0 & p_1 & 0 & -p_2 \\ -p_1 & 0 & p_2 & 0 \\ 0 & -p_3 & 0 & p_4 \\ p_3 & 0 & -p_4 & 0 \end{bmatrix} \begin{bmatrix} \dot{Y} \\ \dot{Z} \\ \dot{\eta} \\ \dot{\zeta} \end{bmatrix} = \begin{bmatrix} (\hat{L}_{1y} - \hat{L}_{2y})/(a_1 + a_2) \\ (\hat{L}_{1z} - \hat{L}_{2z})/(a_1 + a_2) \\ -(a_2 \hat{L}_{1y} + a_1 \hat{L}_{2y})/\Delta \\ -(a_2 \hat{L}_{1z} + a_1 \hat{L}_{2z})/\Delta \end{bmatrix}$$

where

$$p_1 = (A_1 \dot{\theta}_{1x} + A_2 \dot{\theta}_{2x})/(a_1 + a_2)$$

$$p_2 = (a_2 A_1 \dot{\theta}_{1x} - a_1 A_2 \dot{\theta}_{2x})/(a_1 + a_2)^2$$

$$p_3 = (a_2 A_1 \dot{\theta}_{1x} - a_1 A_2 \dot{\theta}_{2x})/\Delta$$

$$p_4 = (a_2^2 A_1 \dot{\theta}_{1x} + a_1^2 A_2 \dot{\theta}_{2x})/(a_1 + a_2)\Delta.$$

## Appendix D

## MATHEMATICAL MODELS USED IN THE 2BODY SIMULATION

## D.1 2BODY MODEL AND COORDINATE SYSTEMS

The two coupled bodies are modeled as two separate rigid bodies connected by a massless joint or hinge as illustrated in Figure D-1. The center of mass (CM) of each body is located relative to an inertial coordinate system by  $\underline{R}_1$  and  $\underline{R}_2$ . Although the simulation assumes that initially (at time = 0),  $\underline{R}_1 = \underline{R}_2 = 0$ , there is no loss of generality. The position vectors  $\underline{d}_1$  and  $\underline{d}_2$  locate the joint or hinge point of each body relative to the center of mass.

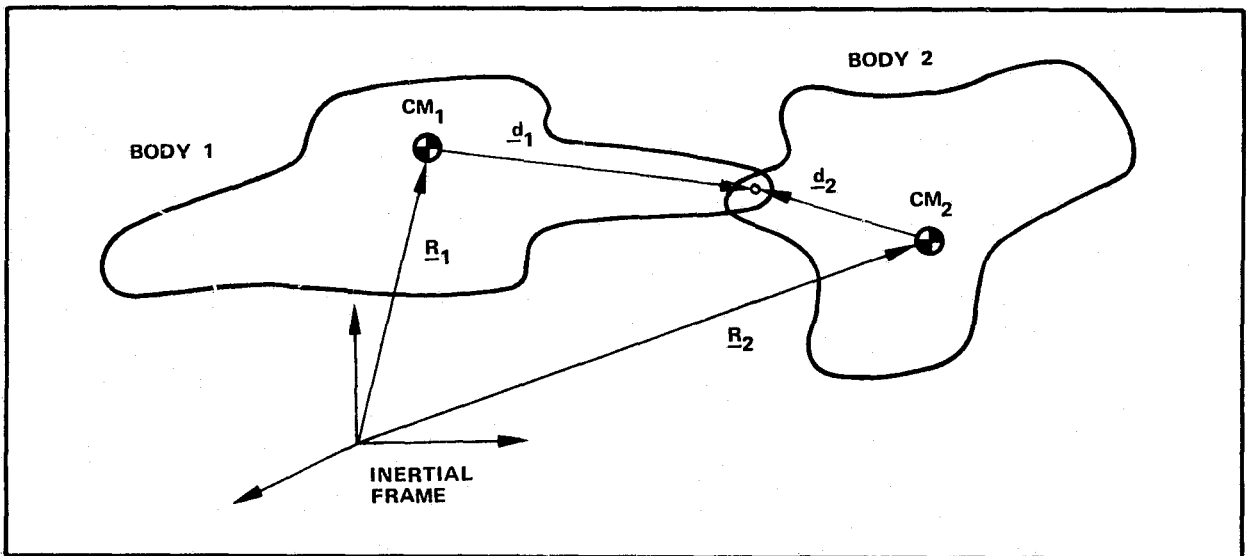


Figure D-1. TWO COUPLED RIGID BODIES INERTIALLY REFERENCED

The relationship between the inertial and body coordinate frames is as follows:

$$\{X\}_I = T_1 \{X\}_1$$

$$\{X\}_I = T_2 \{X\}_2$$

$$\{X\}_1 = T_1^{-1} T_2 \{X\}_2 = T_1^T T_2 \{X\}_2 = T' \{X\}_2$$

The transformation  $T_i$ , ( $i=1,2$ ), is developed from 3-2-1 Euler angle sequence going from the inertial to the body  $i$  reference frame.

The translational and rotational equations of motion are given by

$$\left. \begin{aligned} \ddot{\underline{R}}_i &= \underline{F}_i / m_i \\ \text{and} \\ \underline{I}_i \cdot \dot{\underline{\omega}}_i + \underline{\omega}_i \times \underline{I}_i \cdot \underline{\omega}_i &= \underline{L}_i \end{aligned} \right\} \quad i = 1, 2$$

**D.2 JOINT MODEL/CONSTRAINT AND ALIGNMENT TORQUE**

The joint connecting the two rigid bodies is treated as an ideal docking mechanism during the soft dock regime (the bodies are physically attached, but not yet hard docked (rigidly attached), angular motion can exist between the two vehicles, and the target vehicle could be spinning about an axis close to or coinciding with the docking port axis).

The connection or joint is modeled as a massless spring and damper. From Figure D-2, it is seen that

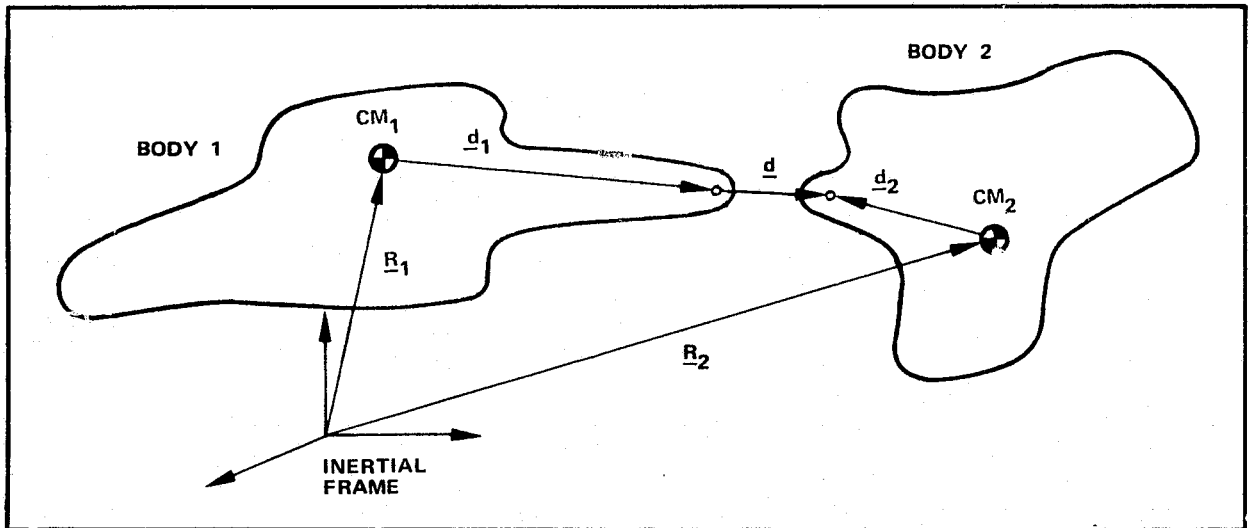


Figure D-2. TWO COUPLED RIGID BODIES WITH IDEAL JOINT

$$\underline{d} = \underline{R}_2 - \underline{R}_1 + \underline{d}_2 - \underline{d}_1$$

and

$$\dot{\underline{d}} = \dot{\underline{R}}_2 - \dot{\underline{R}}_1 + \underline{\omega}_2 \times \underline{d}_2 - \underline{\omega}_1 \times \underline{d}_1$$

where it is assumed that  $|\underline{d}| \ll |\underline{d}_i|, i = 1, 2.$

Initially (at time = 0), however,

$$\underline{d} = \dot{\underline{d}} = 0$$

since the constraint relations

$$\underline{R}_2 = \underline{R}_1 + \underline{d}_1 - \underline{d}_2$$

and

$$\dot{\underline{R}}_2 = \dot{\underline{R}}_1 + \underline{\omega}_1 \times \underline{d}_1 - \underline{\omega}_2 \times \underline{d}_2$$

are used. The joint structure provides a physical constraint force and torque given by

$$\underline{F}_c = K \underline{d} + C \dot{\underline{d}}$$

and

$$\underline{L}_c = \underline{d} \times \underline{F}_c$$

where K and C represent the structural flexibility and damping coefficients. To damp the scissoring-type angular motion between the vehicles, an alignment torque is provided, i.e.,

$$\underline{L}_A = K_A \underline{v} + C_A \dot{\underline{v}}$$

where  $K_A$  and  $C_A$  are spring and damper coefficients and  $\underline{v}$  is an error vector based on the amount of angular misalignment between the docking port axes. The program assumes the x-axes of the vehicles are to be aligned. Thus

$$\underline{v} = \hat{i}_1 \times \hat{i}_2$$

where  $\hat{i}_j$  is the x-axis unit vector of body j, j = 1,2. Since

$$T' = [i_2 | j_2 | k_2] = [T'_{j1} | T'_{j2} | T'_{j3}]$$

then  $\underline{v}$  referenced to the body 1 coordinate frame is

$$\underline{v} = \tilde{i}_1 T'_{j1} = \begin{bmatrix} 0 \\ -T'_{31} \\ T'_{21} \end{bmatrix}$$

where the cross product matrix operator of a general vector

$$\underline{A} = \begin{bmatrix} A_1 \\ A_2 \\ A_3 \end{bmatrix}$$

is formed by

$$\tilde{A} = \begin{bmatrix} 0 & -A_3 & A_2 \\ A_3 & 0 & -A_1 \\ -A_2 & A_1 & 0 \end{bmatrix}$$

Also, then

$$\dot{\underline{v}} = \begin{bmatrix} 0 \\ -\dot{T}'_{31} \\ \dot{T}'_{21} \end{bmatrix}$$

where the elements of  $\dot{\underline{v}}$  can easily be determined from

$$\dot{T}' = T' \tilde{\omega}_2 - \tilde{\omega}_1 T' .$$

To determine values for  $K_A$  and  $C_A$ , the alignment torque is assumed of the form (also a typical rate-position feedback control law)

$$L = I \ddot{\theta} = -K_A \ddot{\theta} - C_A \dot{\theta}$$

where

$I$  - an effective inertia of the system

$\theta$  - a relative angular displacement

$\dot{\theta}$  - a relative angular rate.

Rearranging terms results in

$$\ddot{\theta} + \frac{C_A}{I} \dot{\theta} + \frac{K_A}{I} \theta = 0$$

which is recognized as the equation of motion for a linear harmonic oscillator where

$$\frac{C_A}{I} = 2 \zeta \omega$$



and

$$\frac{K_A}{I} = \omega^2 .$$

Thus

$$K_A = I \omega^2 = 4\pi^2 I f^2$$

and

$$C_A = 2 \zeta I \omega = 4\pi I \zeta f$$

where

f - undamped natural frequency

$\zeta$  - non-dimensional damping factor.

The undamped natural frequency associated with alignment should usually be chosen to be lower than the precessional frequency of the spinning body. The effective inertia can be approximated by that of the reduced inertia of the system, i.e.,

$$I \cong \frac{I_1 I_2}{I_1 + I_2}$$

where  $I_j$  is the inertia of body j, j = 1, 2.

### D.3 DESPIN TORQUER MODEL

When one body is spinning, a torquer is available for despinning. The despin torque can be applied from either body (reflecting actual hardware considerations), but such application is on only the x-axis. For high relative spin rates, the despin torque is limited, providing a constant output, whereas for low relative spin rates the torquer output is linear as seen by the following equations and illustrated in Figure D-3.

$$L_{DX} = \text{sgn}(\omega_{2x} - \omega_{1x}) T_{LIM} , \quad -\Delta\omega > \omega_{2x} - \omega_{1x} > \Delta\omega$$

$$L_{DX} = G(\omega_{2x} - \omega_{1x}) , \quad -\Delta\omega < \omega_{2x} - \omega_{1x} < \Delta\omega$$

The despin torque may be either excluded from the simulation, turned on at time = 0, or activated on an energy condition. The energy condition might

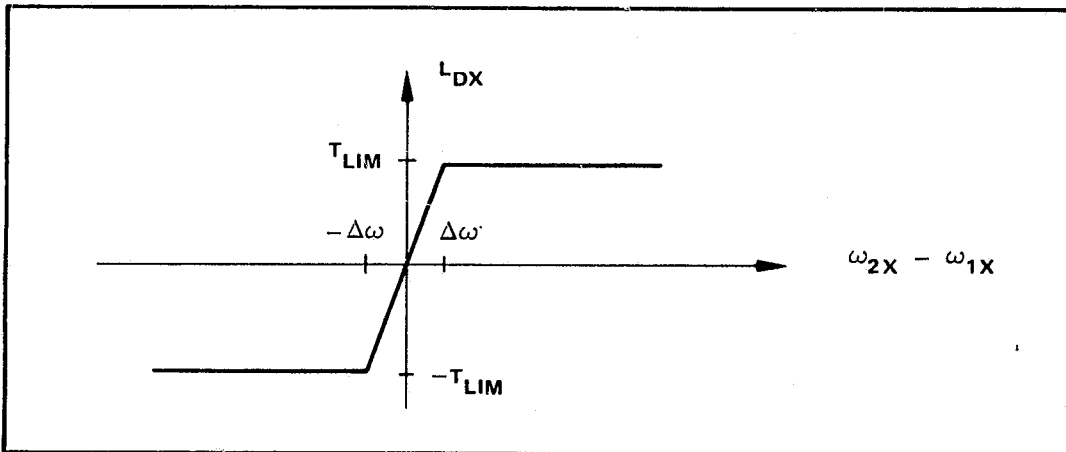


Figure D-3. DESPIN TORQUER OUTPUT MODEL

be desirable if large initial misalignment conditions were used. Only after a highly transient condition damped out would it be appropriate to despin.

#### D.4 BODY 1 ATTITUDE CONTROL

If attitude control of body 1 (usually thought of as the chase vehicle, whereas body 2 is usually thought of as the target and possibly spinning vehicle) is desired, an ideal control system is available. The angular rates of body 1 are continuously set to zero to maintain a fixed vehicle attitude; however, the vehicle is still free to translate.